DIVIDING LINES FOR BACKLASH IN THE PHASE PLANE

WILLIAM J. LUTKENHOUSE

DIVIDING LINES FOR BACKLASH IN THE PHASE PLANE

* * * * * * *

WILLIAM J. LUTKENHOUSE

DIVIDING LINES FOR BACKLASH IN THE PHASE PLANE

by

William J. Lutkenhouse
//
Lieutenant, United States Navy

Submitted in partial fulfillment of
the requirements for the degree of

MASTER OF SCIENCE

IN

ELECTRICAL ENGINEERING

United States Naval Postgraduate School

Monterey, California

1959

DIVIDING LINES FOR BACKLASH

IN THE PHASE PLANE

by

William J. Lutkenhouse

This work is accepted as fulfilling

the thesis requirements for the degree of

MASTER OF SCIENCE

IN

ELECTRICAL ENGINEERING

from the

United States Naval Postgraduate School

ABSTRACT

The phase plane, or displacement versus velocity plane, while relatively new to the engineering field, is particularly suited to furnishing a comprehensive graphical display of nonlinearities operating under certain conditions.

Although a successive phase plane application is required to display a system of order greater than two, a one picture phase plane presentation is adequate for predicting the stability and transient performance of a second order system.

Backlash effects are investigated by phase plane techniques in this thesis.

The writer wishes to express his appreciation to Dr. George J. Thaler, without whose assistance and encouragement, this thesis would not have been written.

TABLE OF CONTENTS

LIST OF ILLUSTRATIONS

1. Backlash

Backlash is a real engineering problem. It exists in all gear trains to a greater or lesser extent and in multiple gear arrangements, is the sum of the backlash errors of the individual gears. Dependent upon where the servo mechanism error is measured, backlash contributes either to the steady state error, or instability of the system. Backlash is not always detrimental to system performance for when controlled, can be used to introduce a slight "dither" to a system, which may be used to provide good lubrication and freedom from stictional effects.

The second order system consisting of motor and load is treated as two linear systems operating sequentially (a) during the period when the backlash is taken up and the load is being driven by the motor and (o) when the load is drifting separately in the backlash region with the motor being controlled by an error signal generated from output measured at either load shaft or motor shaft. Both locations of output measurement are considered.

2. Dividing Lines

System response may be predicted on the phase plane by the loci of four dividing lines in conjunction with system isoclines: (a) system separation line (b) velocity and displacement of system without load at time of recombination (c) velocity and displacement of load at time of recombination (d) velocity and displacement of recombined system after momentum conservation conditions have been satisfied.

This study treats all recombinations as being inelastic.

When an error exists in a system, and the system is correcting with the backlash taken up, a decelerating torque must eventually be applied to the motor. At some time afterward, providing viscous friction is not infinite at the load, and that coulomb friction of load can be neglected, the velocities of the motor and load become different, mechanical contact is lost and separation occurs. This line of separation is a straight line consisting of that isocline or constant slope line at which the load trajectory and the trajectory of the system with load removed, have a common slope. It may be called the "Separation dividing line". Past the separation dividing line, the system operates in the backlash region during which time the load drifts separately, with undiminished velocity if its viscous friction is negligible or with a constant deceleration presuming all friction is viscous. The remainder of the system acts as a stable system with decreased inertia and spirals in towards a stable focus if system output is measured at motor shaft. If the system output is measured at the drifting load, the system does not behave stably in the backlash region but continues to drive in the reverse direction until the backlash has taken up and system output completely

corrected as to displacement. From this it may be seen that when the system output is measured at the drifting load, backlash between motor and load may make an overdamped system oscillatory.

The initial position of system velocity and displacement on the separation dividing line determines two points on the phase plane, load velocity and displacement at instant of recombination, and system without load velocity and displacement at instant of recombination. The loci of these two points constitute dividing lines listed in (b) and (c) above. Each pair of corresponding points for load and system without load, velocity and displacement at recombination, in turn determine a point on the locus for recombined system velocity and displacement. This final point is obtained from satisfying the conservation of momentum considerations where individual momentums are defined for load and system without load. Trajectories for the recombined system originate from this final dividing line and the system retains its original characteristics until the next separation dividing line is reached, after which, separation and recombination occur as in the previous half cycle.

If in response to a step displacement, the system attains a quiescent condition, with or without steady state displacement error, the system is said to be stable.

If the final state of the system is one of a constant amplitude oscillation, the system is said to have a limit cycle. The magnitude of this limit cycle may be determined by any of the possible non linearities of the system, dead zone, etc. but in this thesis, only limit cycles resulting from backlash are considered.

3. Output measured at motor shaft, load having viscous friction.

Consider first, the system in which the output measuring device is mounted on the motor shaft. The backlash existing in the gear train between motor and load is outside of the feedback loop as shown in "Fig.1". The closed loop is completely linear. Ultimate stability with a steady state displacement error less than or equal to the amount of the backlash is the result. The drifting load can at most store energy and since the load does not determine the output measurement, it does not demand more power from the source than is required. The combined viscous friction of the load and the system without load represent energy dissipations which insure stability.

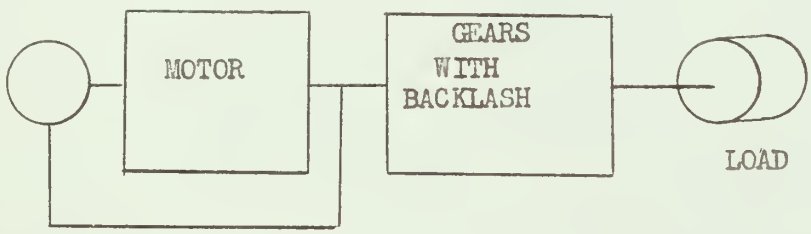

Figure (1)

When the backlash is taken up, the differential equations for the system are:

(1) $\frac{1}{N}\left(N^2 J_m + J_L\right)\ddot{\theta}_o + \frac{1}{N}\left(N^2 f_m + f_L\right)\dot{\theta}_o = T$

(2) $T = K_1 I$

(3) $V = RI + K_2 \dot{\theta}_m$

(4) $$I = \left(\frac{V}{R} - \frac{K_2}{R} N \dot{\theta}_o \right)$$

(5) $$V = K_3 \left(\theta_R - \theta_o \right)$$

(6) $$\frac{1}{N} \left(N^2 J_m + J_L \right) \ddot{\theta}_o + \frac{1}{N} \left(N^2 f_m + f_L + \frac{K_1 K_2 N^2}{R} \right) \dot{\theta}_o + \frac{K_1 K_3}{R} \theta_o = \frac{K_1 K_3}{R} \theta_R$$

Where

K_1 = motor torque constant $\frac{\text{ft. lbs.}}{\text{amp.}}$

K_2 = motor generator constant $\frac{\text{volts}}{\text{rad./sec.}}$

K_3 = error measurement constant $\frac{\text{volts}}{\text{rad.}}$

R = armature resistance

N = gear ratio $\frac{\text{rad. motor}}{\text{rad. output}}$

J_m = inertia of system without load $\frac{\text{ft. lbs.}}{\text{rad./sec.}^2}$

$N f_m + \frac{K_1 K_2}{R} N = F_m$ = friction of system without load

$\frac{K_1 K_3}{R} = K$

$\frac{f_L}{N} = F_L$

θ_R = ordered displacement

θ_L = displacement of load

θ_o = displacement of combined system

θ_m = displacement of system without load

Letting $N = 1$ $\theta_R = 1$

From equation (6), to obtain the equation for the isoclines of the combined system:

(7) $$\ddot{\theta}_o + \left(\frac{F_m + F_L}{J_m + J_L} \right) \dot{\theta}_o = \left(\frac{K}{J_m + J_L} \right) \left(1 - \theta_o \right)$$

Letting $\frac{\ddot{\theta}_o}{\dot{\theta}_o} = \eta_1 =$ slope of trajectory at isocline

$$(8) \quad \theta_o = 1 - \dot{\theta}_o \left(\frac{\eta_1 + \frac{F_m + F_L}{J_m + J_L}}{K / J_m + J_L} \right)$$

When the system with load removed constitutes a closed system, an equation for the isoclines may be written as follows:

$$(9) \quad J_m \ddot{\theta}_m + F_m \dot{\theta}_m = K(1 - \theta_m)$$

$$(10) \quad \theta_m = 1 - \dot{\theta}_m \left(\frac{\eta_2 + \frac{F_m}{J_m}}{K / J_m} \right)$$

Where $\eta_2 = \frac{\ddot{\theta}_m}{\dot{\theta}_m}$

Under deceleration conditions, when the velocity of the system without load is equal to the velocity of the load drifting separately, separation occurs and the backlash becomes operative. The isocline for the drifting load is determined by the friction and inertia of the load.

$$(11) \quad J_L \ddot{\theta}_L + F_L \dot{\theta}_L = 0$$

$$(12) \quad \frac{\ddot{\theta}_L}{\dot{\theta}_L} = -\frac{F_L}{J_L} = \eta_3$$

To prove that the system remains combined until it reaches the isocline of the system without load which has the same slope as the load trajectory, consider the following, assuming that $\eta_1 = \eta_2 = 0$ as shown in "Fig. 2" :

Figure (2)

(13) $$\frac{\dot{\theta}_o}{\theta_o} = \frac{K}{F_m + F_L}\left(\frac{1}{\theta_o} - 1\right)$$

(14) $$\frac{\dot{\theta}_m}{\theta_m} = \frac{K}{F_m}\left(\frac{1}{\theta_m} - 1\right)$$

where $\theta_{oc} = \theta_{mc}$ at time of separation

Since $$\left|\frac{\dot{\theta}_m}{\theta_m}\right| \gg \left|\frac{\dot{\theta}_o}{\theta_o}\right|$$

if separation is attempted when η_1 for the combined system isocline is equal to η_3 for the drifting load, the motor will accelerate, keeping the system combined until η_2 for the system without load is common with η_3 of the drifting load.

To find the loci for the dividing lines:

(a) system without load velocity and displacement at recombination,

(b) load velocity and displacement at time of recombination, the equations of the individual systems are solved as linear equations, using initial conditions determined from θ_o $\dot{\theta}_o$ on the separation dividing lines, and final conditions determined by the amount of backlash to be taken up.

For the combined system:

(15) $$\left(J_m + J_L\right)\ddot{\theta}_o + \left(F_m + F_L\right)\dot{\theta}_o + K\theta_o = K\theta_R$$

For the system with load removed:

$$J_m \ddot{\theta}_m + F_m \dot{\theta}_m + K\theta_m = K\theta_R \tag{16}$$

For the load drifting separately

$$J_L \ddot{\theta}_L + F_L \dot{\theta}_L = 0 \tag{17}$$

At separation

$\theta_{mo} = \theta_{Lo} = \theta_{oo}$ = displacement of system with/without load

$\dot{\theta}_{mo} = \dot{\theta}_{Lo} = \dot{\theta}_{oo}$ = velocity of system with/without load

Putting these conditions into the system with load removed and solving yields:

$$\theta_m\left(s^2 + \frac{F_m}{J_m}s + \frac{K}{J_m}\right) = \frac{K\theta_R}{s J_m} + s\theta_{mo} + \frac{F_m}{J_m}\theta_{mo} + \dot{\theta}_{mo} \tag{18}$$

Since the isoclines are straight lines, $\dfrac{\dot{\theta}_{mo}}{\theta_{mo} - \theta_R} = \tan\phi$

where ϕ is the angle the common load, system without load isocline makes with the positive $\theta_o > \theta_R$ axis. θ_{mo} may be expressed in terms of $\dot{\theta}_{mo}$ as

$$\theta_{mo} = \theta_R + \frac{\dot{\theta}_{mo}}{\tan\phi} \tag{19}$$

Equation (18) then reduces to

$$(20)\quad \theta_m = \frac{K\theta_R}{s\left(s^2 + \frac{F_m}{J_m}s + \frac{K}{J_m}\right)} + \frac{\left(\theta_R + \frac{\dot{\theta}_{mo}}{\tan\phi}\right)\left(s + \frac{F_m}{J_m}\right) + \dot{\theta}_{mo}}{\left(s^2 + F_m/J_m\, s + K/J_m\right)}$$

$$(21)\quad \dot{\theta}_m = \frac{K\theta_R}{\left(s^2 + \frac{F_m}{J_m}s + \frac{K}{J_m}\right)} + \frac{s\left(\theta_R + \frac{\dot{\theta}_{mo}}{\tan\phi}\right)\left(s + \frac{F_m}{J_m}\right) + s\,\dot{\theta}_{mo}}{\left(s^2 + \frac{F_m}{J_m}s + \frac{K}{J_m}\right)}$$

For the load only, imposing initial conditions yields:

$$(22)\quad \theta_L = \frac{\left(\theta_R + \frac{\dot{\theta}_{Lo}}{\tan\phi}\right)\left(s + \frac{F_L}{J_L}\right) + \dot{\theta}_{Lo}}{s\left(s + F_L/J_L\right)}$$

$$(23)\quad \dot{\theta}_L = \frac{\dot{\theta}_{Lo}}{\left(s + F_L/J_L\right)}$$

When recombination occurs, neglecting elastic bounce of gear teeth, $\dot{\theta}_m$ and $\dot{\theta}_L$ change instantaneously in accordance with the law of conservation of momentum, to satisfy the following equation:

$$(24)\quad \left(J_m + J_L\right)\dot{\theta}_o = J_m\,\dot{\theta}_m + J_L\,\dot{\theta}_L$$

The loci of the dividing lines for θ_m, $\dot{\theta}_m$, θ_L, $\dot{\theta}_L$,

θ_c , $\dot{\theta}_c$ at recombination are obtained as follows:

Equations (20) and (22) are solved as a function of time and plotted with an arbitrary ordinate scale, for example let 1 in. ordinate displacement = 1 rad., as in "Fig. 3", which is representative of any system where backlash is outside the feedback loop.

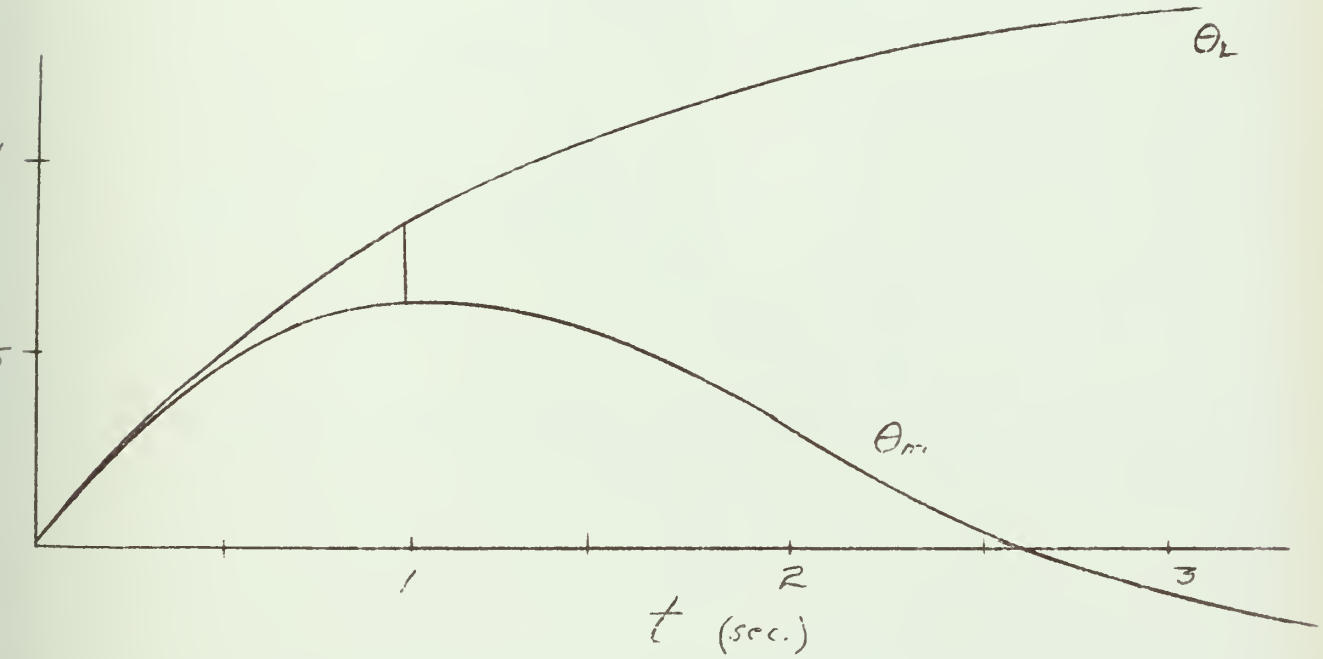

Figure (3)

To find time (t) at which .2 rad. backlash is taken up given an initial condition of $\dot{\theta}_{Lc}$ = .5, proceed as follows: Since above figure was plotted using $\dot{\theta}_{Lo}$ as a parameter with 1 rad. = 1 in., let ordinate = scale of 1 rad = 2 in. = $^1/_{.5}$ . .2 rad. backlash represented by separation between θ_L and θ_m, is now equal to .4 in. With dividers, fit .4 in. to time (t) for recombination. (t) is found to be .95 sec

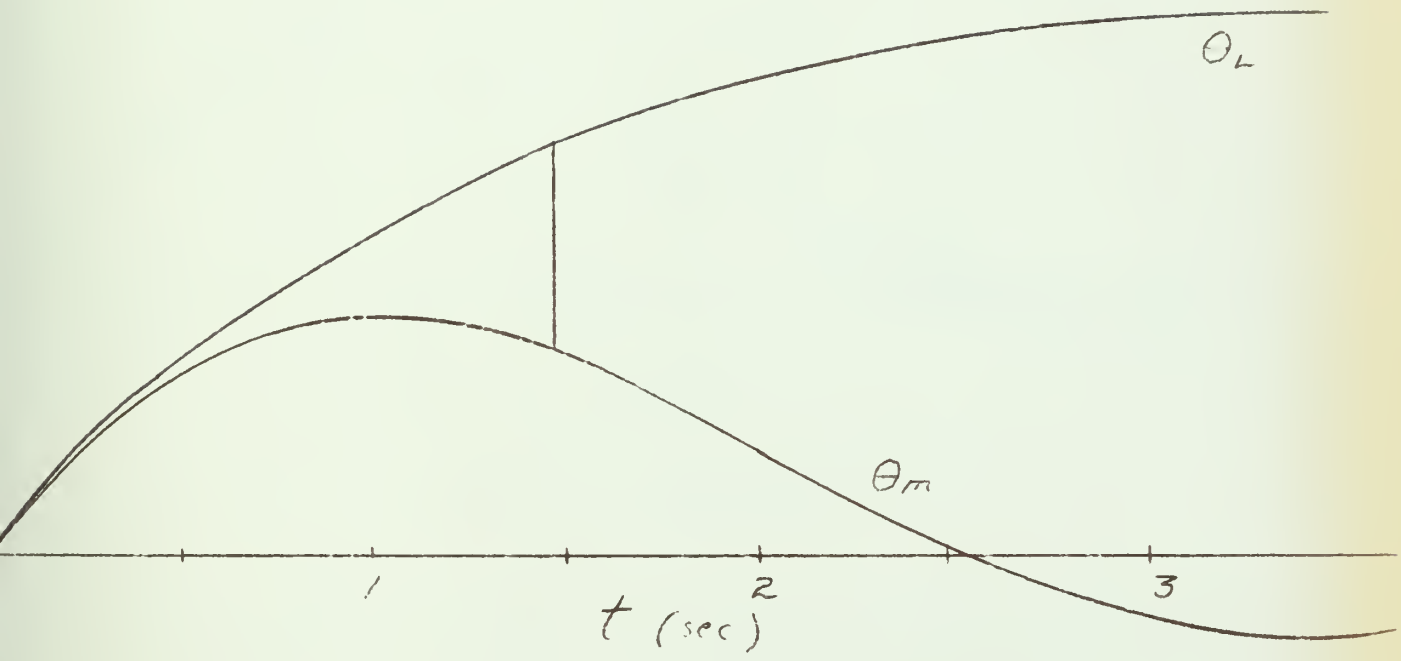

Figure (4)

To find time (t) at which . 2 rad. backlash is taken up given an initial condition of $\dot{\theta}_{L_0} = .2$, let ordinate scale be 1 rad. = 5 in. or 1 in. = . ? rad. Backlash of .2 rad is now equal to 1 in. With dividers fit 1 in. between θ_L and θ_m, read (t) on abscissa equal to 1.45 sec.

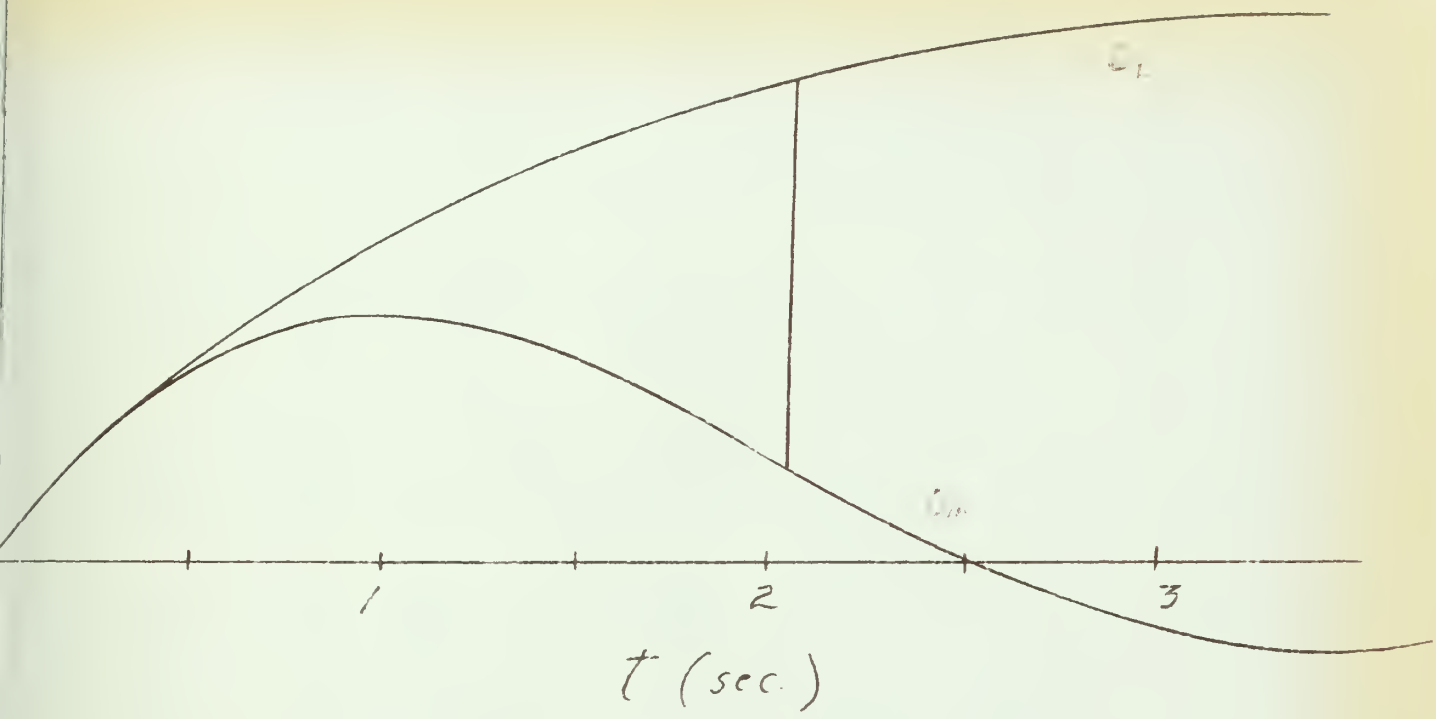

Figure (5)

To find time (t) at which . 2 rad backlash is taken up given an initial condition of $\dot{\theta}_{L_0} = .1$, let ordinate scale be 1 rad. = 10 in. or 1 in. = . 1 rad. Backlash of . 2 rad is now equal to 2 in. With dividers fit 2 in. between θ_L and θ_m, read (t) on abscissa at 2.05 sec.

Complete loci of dividing lines are obtained by substituting values of (t) obtained from initial conditions of $\dot{\theta}_{L_0}$, into equations (20), (21), (22), and (23). Resulting values of θ_m, $\dot{\theta}_m$, θ_L, $\dot{\theta}_L$ are then plotted on the phase plane. θ_o and $\dot{\theta}_o$ are obtained by substituting values of $\dot{\theta}_m$ and $\dot{\theta}_L$, from equations (21) and (23) into equation (24), for corresponding times.

In the case where output is measured at the motor shaft, upon recombination is equal to the displacement of θ_m. When system output is measured at the load, θ_o upon recombination is equal to the displacement of θ_L.

4. Stability

A spot check of stability may be made at any particular recombination point by treating the phase plane trajectories as logarithmic spirals with transformations as follow:

For the combined system let $J_m + J_L = J$, $F_m + F_L = F$

(25) $$J\ddot{\theta}_o + F\dot{\theta}_o + K\theta_o = K\theta_R$$

(26) $$\frac{\ddot{\theta}_o}{\dot{\theta}_o} = \frac{\frac{K\theta_R}{J} - \frac{K\theta_o}{J}}{\dot{\theta}_o} - \frac{F}{J}$$

(27) Let $\dot{\theta}_o = u(\theta_R - \theta_o)$

(28) $$d\dot{\theta}_o = (\theta_R - \theta_o)\,du - u\,d\theta_o$$

(29) $$(\theta_R - \theta_o)\,du = u + \frac{K/J}{u} - F/J$$

(30) $$\int \frac{d\theta_o}{(\theta_R - \theta_o)} = \int \frac{u\,du}{u^2 - F/J\,u + K/J}$$

(31) $$-\ln(\theta_R - \theta_o) = \int \frac{u\,du}{(u - F/2J)^2 + \left(K/J - F^2/4J^2\right)}$$

(32) Let $$(u - F/2J) = \sqrt{K/J - F^2/4J^2}\,\tan z$$

(33) $$du = \sqrt{K/J - F^2/4J^2}\,\sec^2 z\,dz$$

(34) $$-\ln(\theta_R - \theta_o) = \int \frac{\left(\sqrt{K/J - \frac{F^2}{4J^2}}\tan z + \frac{F}{2J}\right)\left(\sqrt{K/J - \frac{F^2}{4J^2}}\sec^2 z\,dz\right)}{\left(\frac{K}{J} - \frac{F^2}{4J^2}\right)\sec^2 z}$$

$$= \ln\cos z + \frac{F/2J}{\sqrt{\frac{K}{J} - \frac{F^2}{4J^2}}}\arctan\frac{u - F/2J + C}{\sqrt{\frac{K}{J} - \frac{F^2}{4J^2}}}$$

$$\cos Z = \sqrt{\frac{K/J - F^2/4J^2}{u^2 - F/J\,u + K/J}} \tag{35}$$

$$-\ln(\theta_R - \theta_o) = -\ln\sqrt{\frac{K/J - F^2/4J^2}{u^2 - F/J\,u + K/J}} + \frac{F/2J}{\sqrt{K/J - \frac{F^2}{4J^2}}} \arctan \frac{u - F/2J + C}{\sqrt{K/J - F^2/4J^2}} \tag{36}$$

$$\dot{\theta}_o^{\,2} - F/J\,\dot{\theta}_o(\theta_R - \theta_o) + K/J\,(\theta_R - \theta_o)^2 = C^2\left(K/J - \frac{F^2}{4J^2}\right) e^{\frac{-F/2J}{\sqrt{K/J - F^2/4J^2}} \arctan \frac{\dot{\theta}_o - F/2J(\theta_R - \theta_o)}{(\theta_R - \theta_o)\sqrt{K/J - F^2/4J^2}}} \tag{37}$$

To determine if a particular recombination point on a trajectory is approaching stability (i.e., the recombined trajectory is closer to the stable focus than prior to separation), it is necessary to compare values of C obtained from the coordinates of the trajectory where separation occurs and from the coordinates, where recombination occurs, the conservation of momentum criteria having been first satisfied.

$$C = \left(\sqrt{\frac{\dot{\theta}_o^{\,2} - F/J\,\dot{\theta}_o(\theta_R - \theta_o) + K/J\,(\theta_R - \theta_o)^2}{K/J - F^2/4J^2}}\right) \cdot \left(e^{\frac{F/2J}{\sqrt{K/J - F^2/4J^2}} \arctan \frac{\dot{\theta}_o - F/2J(\theta_R - \theta_o)}{(\theta_R - \theta_o)\sqrt{K/J - F^2/4J^2}}}\right) \tag{38}$$

If C ($\theta_o, \dot{\theta}_o$) recombined $>$ C ($\theta_i, \dot{\theta}_i$) unseparated, the trajectory will diverge into a limit cycle. This comparison of values of C is illustrated in Fig. 6. This method is applied to test limit cycles developed in cases III and IV.

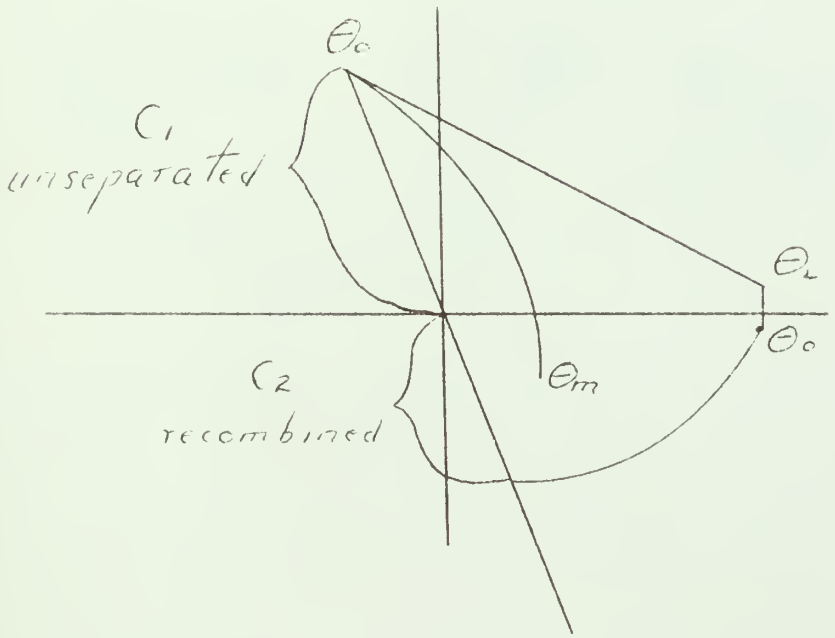

Figure (6)

5. Output measured at load, load having viscous friction.

When the backlash is placed inside the feedback loop, i.e., when the output is measured at the load, the configuration of the system is as illustrated in Fig. 7.

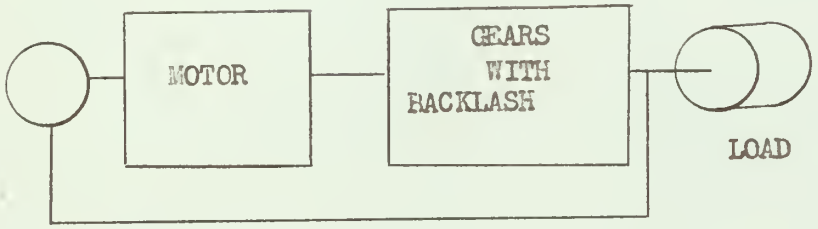

Figure (7)

In the combined region, behavior of the system is identical to that of the system described in section three; however, the system with load removed, as it is when in the backlash region, is no longer a closed system. The system with load removed is driven open loop and attempts to correct the error as usual. It is prevented from doing so by the existence of backlash. In this attempt, the inertia of the system with load removed develops a momentum which in an underdamped system always causes instability and a consequent limit cycle, but for the presence of coulomb friction.

Equation (9) reduces to

$$J_m \ddot{\theta}_m + F_m \dot{\theta}_m = K(\theta_R - \theta_L) \tag{39}$$

Since from equation (22), θ_L in La Place form is equal to

$$\frac{\left(\theta_R + \frac{\dot{\theta}_{L0}}{\tan\phi}\right)\left(s + F_L/J_L\right) + \dot{\theta}_{L0}}{s\left(s + F_L/J_L\right)}$$

equation (20) is reduced to

$$(40)\quad \theta_m = \frac{K/J_m\left(-\frac{\dot\theta_{mo}}{\tan\phi}\right)}{s^2\left(s+F_m/J_m\right)} - \frac{K/J_m\,\dot\theta_{mo}}{s^2\left(s+F_m/J_m\right)\left(s+F_L/J_L\right)} + \frac{\dot\theta_{mo}}{s\left(s+F_m/J_m\right)} + \frac{1+\frac{\dot\theta_{mo}}{\tan\phi}}{s}$$

$$(41)\quad \dot\theta_m = \frac{K/J_m\left(-\frac{\dot\theta_{mo}}{\tan\phi}\right)}{s\left(s+F_m/J_m\right)} - \frac{K/J_m\,\dot\theta_{mo}}{s\left(s+\frac{F_m}{J_m}\right)\left(s+\frac{F_L}{J_L}\right)} + \frac{\dot\theta_{mo}}{\left(s+\frac{F_m}{J_m}\right)}$$

Since the system with load removed is not suitable for the isocline method, a time solution of equations (40) and (41) is required.

A plot of t versus θ_m and θ_L result in a graph similar to Fig. 8 and is used as previously described in section three to give values of (t) for computation of θ_m, $\dot\theta_m$, θ_L, $\dot\theta_L$, θ_o, $\dot\theta_o$ dividing lines.

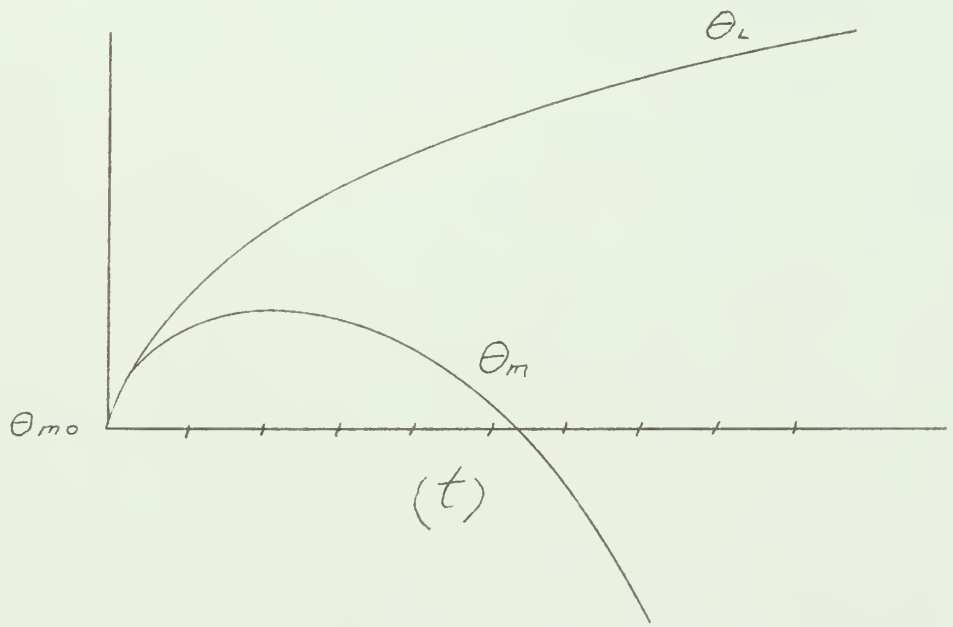

Figure (8)

6. Case I. Output measured at motor shaft.

Given system

Combined

(42) $1\ddot{\theta}_o + .8\dot{\theta}_o + \theta_o = 1$

System with load separated

(43) $.6\ddot{\theta}_m + .48\dot{\theta}_m + \theta_m = 1$

Load

(44) $.4\ddot{\theta}_L + .32\dot{\theta}_L = 0$

Backlash . 2 rad.

Isocline at which load separates from system is determined from load equation.

(45) $\frac{\ddot{\theta}_L}{\dot{\theta}_L} = \eta_3 = -\frac{.32}{.4} = -.8$

To find isoclines of combined system letting $\theta_R = 1$

(46) $\eta_1 + .8 = \frac{1 - \theta_o}{\dot{\theta}_o}$

Computed values of arctan $\frac{\dot{\theta}_o}{1 - \theta_o}$ for various values of N. are as listed in table one.

Table (1)

N_1	Arctan $\frac{\dot{\theta}_o}{1-\theta_o}$	N_1	Arctan $\frac{\dot{\theta}_o}{1-\theta_o}$
10	- 5.30°	- .2	- 59°
7	- 7.31°	- .3	- 63.4°
5	- 9.78°	- .5	- 73.3°
3	-14.75°	- .7	- 84.3°
2	-19.65°	- .8	90°
1.5	-23.5°	- 1	78.7°
1	-29.05°	- 1.2	68.2°
.7	-33.7°	- 1.5	55°
.5	-37.6°	- 1.7	48°
. 3	-42.25°	- 2	39.8°
.2	-45°	- 2.5	30.45°
.1	-48°	- 3	24.45°
0	-51.35°	- 5	13.39°
.1	-55°	- 7	9.15°
		-10	6.20°

To find isoclines of system with load separated

$$(47)\quad \eta_2 + .8 = \frac{1.66\,(1-\theta_m)}{\dot{\theta}_m}$$

Table (2)

N_2	arctan $\frac{\dot{\theta}_m}{1-\theta_m}$	N_2	arctan $\frac{\dot{\theta}_m}{1-\theta_m}$
10	- 7.04°	- .7	- 85.7°
7	- 9.7°	- .8	- 90°
5	- 12.95°	- 1	81.45°
3	- 19.35°	- 1.5	62.3°
2	- 25.5°	- 2	48°
1	- 36.5°	- 2.5	38.1°
1.5	- 30.1°	- 3	31.2°
.7	- 41.6°	- 5	17.62°
.5	- 45.75°	- 7	12.13°
.3	- 50.45°	- 10	8.25°
.2	- 51.13°		
.1	- 55.95°		
0	- 59°		
-.1	- 62.3°		
-.2	- 65.8°		
- .3	- 69.45°		
-.5	- 77.31°		

To obtain loci for $\theta_m \dot{\theta}_m$, $\theta_L \dot{\theta}_L$ dividing lines, it is necessary to solve equations for θ_m, θ_L using initial conditions determined from separation dividing line of $\eta_2 = -.8$

(48) $$\ddot{\theta}_m + .8\dot{\theta}_m + 1.666\,\theta_m = 1.666$$

In LaPlace form

(49) $$\theta_m = \frac{\frac{1.666}{s} + s\theta_{mo} + .8\theta_{mo} + \dot{\theta}_{mo}}{(s^2 + .8s + 1.666)}$$

Roots of quadratic factor are $-.4 \pm j\,1.225$

(50) $$\theta_m = \frac{1666}{s(s + .4 \pm j1.225)} + \frac{\theta_{mo}(s + .8) + \dot{\theta}_{mo}}{(s + .4 \pm j\,1.225)}$$

(51) $$\theta_m = 1 + \frac{\dot{\theta}_{mo}}{1.225} e^{-.4t} \sin 1.225t$$

(52) $$\dot{\theta}_m = -\frac{\dot{\theta}_{mo}}{1.225} e^{-.4t} \sin 1225t + \dot{\theta}_{mo} e^{-.4t} \cos 1.225t$$

For load separately

In La Place Form

(53) $$\theta_L = \frac{\dot{\theta}_{mo}}{s(s+.8)} + \frac{\theta_{mo}}{s}$$

(54) $$\theta_L = \frac{\dot{\theta}_{mo}}{.8}\left(1 - e^{-.8t}\right) + \theta_{mo}$$

(55) $$\dot{\theta}_L = \dot{\theta}_{mo} e^{-.8t}$$

Equations (51) and (54) are evaluated at times indicated from factors listed in Table three. These equations are then plotted for $\dot{\theta}_{mo}$ of .1 to produce a graph similar to Fig. 3., from which values of time for recombination are obtained for various initial values of $\dot{\theta}_{mo}$.

Table 3

t	$\sin 1.225t$	$e^{-.4t}$	$e^{-.8t}$	θ_m	θ_L
.1	.1222	.9608	.9232	.0096	.0096
.2	.2425	.9231	.8545	.0183	.0183
.4	.4706	.8521	.7260	.0328	.03425
.6	.6706	.7866	.6190	.0431	.0476
.8	.8305	.7260	.5275	.0493	.059
1.0	.9408	.6700	.4500	.0515	.0688
1.2	.9949	.6188	.3830	.0503	.077
1.5	.9642	.5490	.3015	.0432	.0873
1.8	.8070	.4865	.2370	.0321	.0955
2.0	.6377	.4490	.2020	.0234	.0955
2.2	.4275	.4145	.1720	.0145	.1035
2.3	.3175	.3985	.1590	.0103	.105
2.5	.0750	.3680	.1355	.0023	.108
2.6	-.0436	.3540	.1250	-.0013	.1095
2.8	-. 289	.3260	.1063	-.0077	.1115
3.2	-. 200	.2780	.0770	-.0159	.1153
3.5	-. 910	.2460	.0608	-.0183	.1175
3.9	-.9975	.2100	.0440	-.0171	.1194

From plotting and scaling as described in section three, it was determined that .2 rad. backlash was taken up at times indicated in Table four corresponding to initial separation values of $\dot{\theta}_{mo}$ as indicated. Values of θ_m $\dot{\theta}_m$ θ_L $\dot{\theta}_L$ were obtained from substitution of values of $\dot{\theta}_{mo}$ and t, in equations (51) (52), (54) and (55). Values of $\dot{\theta}_o$ were obtained from substituting values of $\dot{\theta}_m$ and $\dot{\theta}_L$ into equation (24).

Table 4

$\dot{\theta}_{mo}$	t	θ_m	$\dot{\theta}_m$	θ_L	$\dot{\theta}_L$	$\dot{\theta}_o$ recombined
.9	1.1	1.460	-.0594	1.660	.372	.1150
.8	1.175	1.406	-.0945	1.607	.3135	.0648
.7	1.23	1.348	-.1114	1.548	.262	.0379
.6	1.32	1.288	-.1304	1.489	.208	.0055
.5	1.44	1.226	-.1417	1.426	.159	-.0213
.4	1.59	1.161	-.1422	1.360	.112	-.0405
.3	1.825	1.080	-.1264	1.289	.0697	-.0331
.2	2.35	1.013	-.0812	1.213	.0298	-.0368
.13	2.7	-.0605	-.0195	1.1436	.0151	-.0057

Dividing lines were plotted on the phase plane of the system shown in Fig. 9. Phase trajectories were formed by standard phase plane techniques. The transient response of the system as obtained from the phase plane by methods outlined in Control System Synthesis by Truxal, page 629, is shown in Fig. 10. Values of displacement versus time for transient response are listed in Table five.

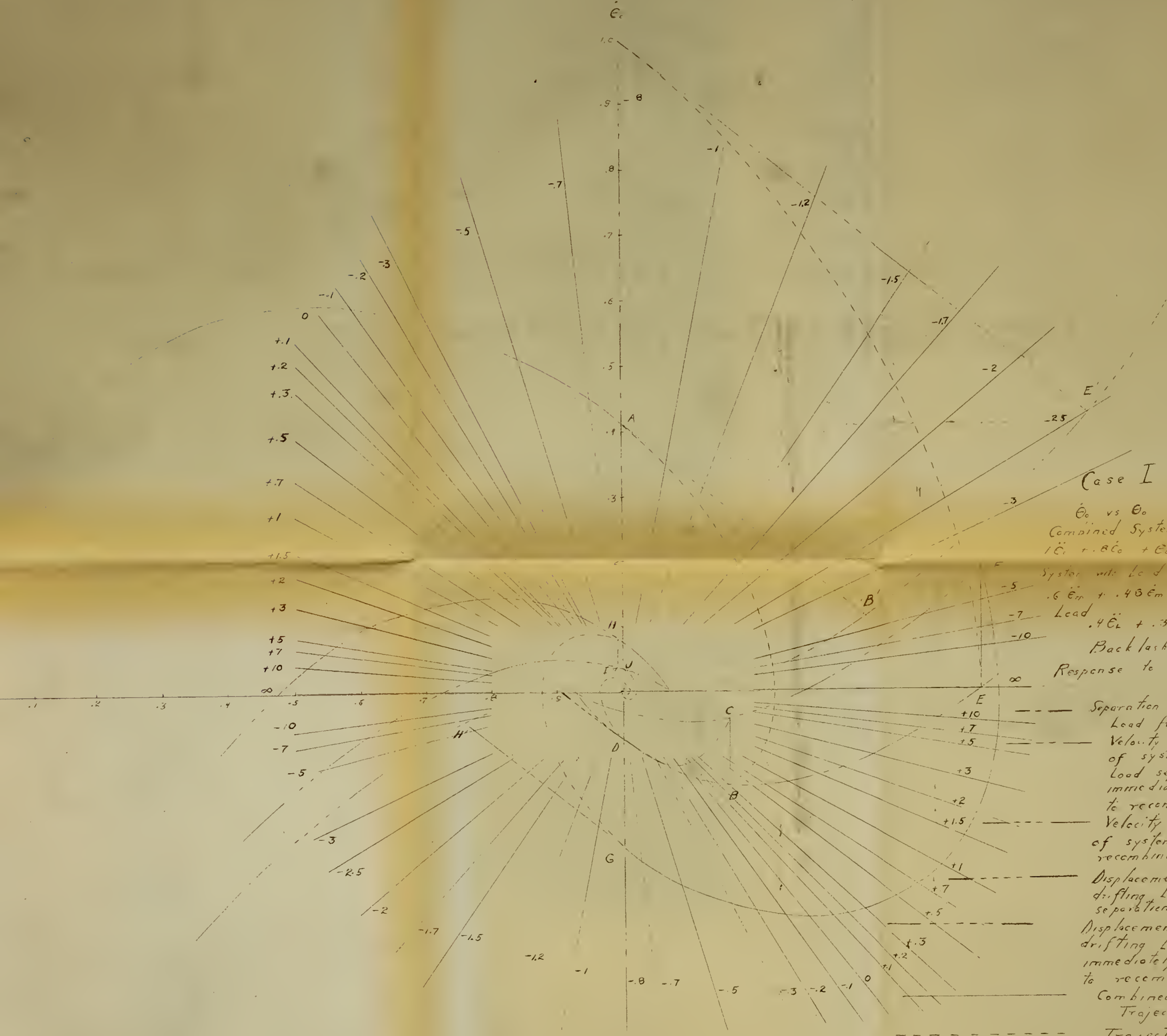
$\dot{e}_c$
1.0
.9
.8
.7
.6
.5
.4
.3
A
B
B'
C
D
E
E'
F
G
H
J
K
-.1
0
+.1
+.2
+.3
+.5
+.7
+1
+1.5
+2
+3
+5
+7
+10
∞
-.2
-.3
-.5
-.7
-1
-1.2
-1.5
-1.7
-2
-2.5
-3
-5
-7
-10
.1
.2
.3
.4
.5
.6
.7
.8
Case I
$\dot{\theta}_o$ vs θ_o
Combined System
$1\ddot{e}_c + .8\dot{e}_c + e_c = 1$
System with Lead Separated
$.6\ddot{e}_m + .48\dot{e}_m + e_m = 1$
Lead
$.4\ddot{e}_L + .32\dot{e}_L = e$
Backlash .2 rad
Response to step of 1, $1\dot{e}_c$
Separation Line
Lead from system Velocity and displacement of system with Load separated immediately prior to recombination
Velocity and displacement of system upon recombination
Displacement and velocity drifting Load during separation
Displacement and velocity drifting Load immediately prior to recombination
Combined System Trajectory
Trajectory of System with Load separated
Numbered Isoclines

Figure 9.

Case I

Transient Response
to unit step input

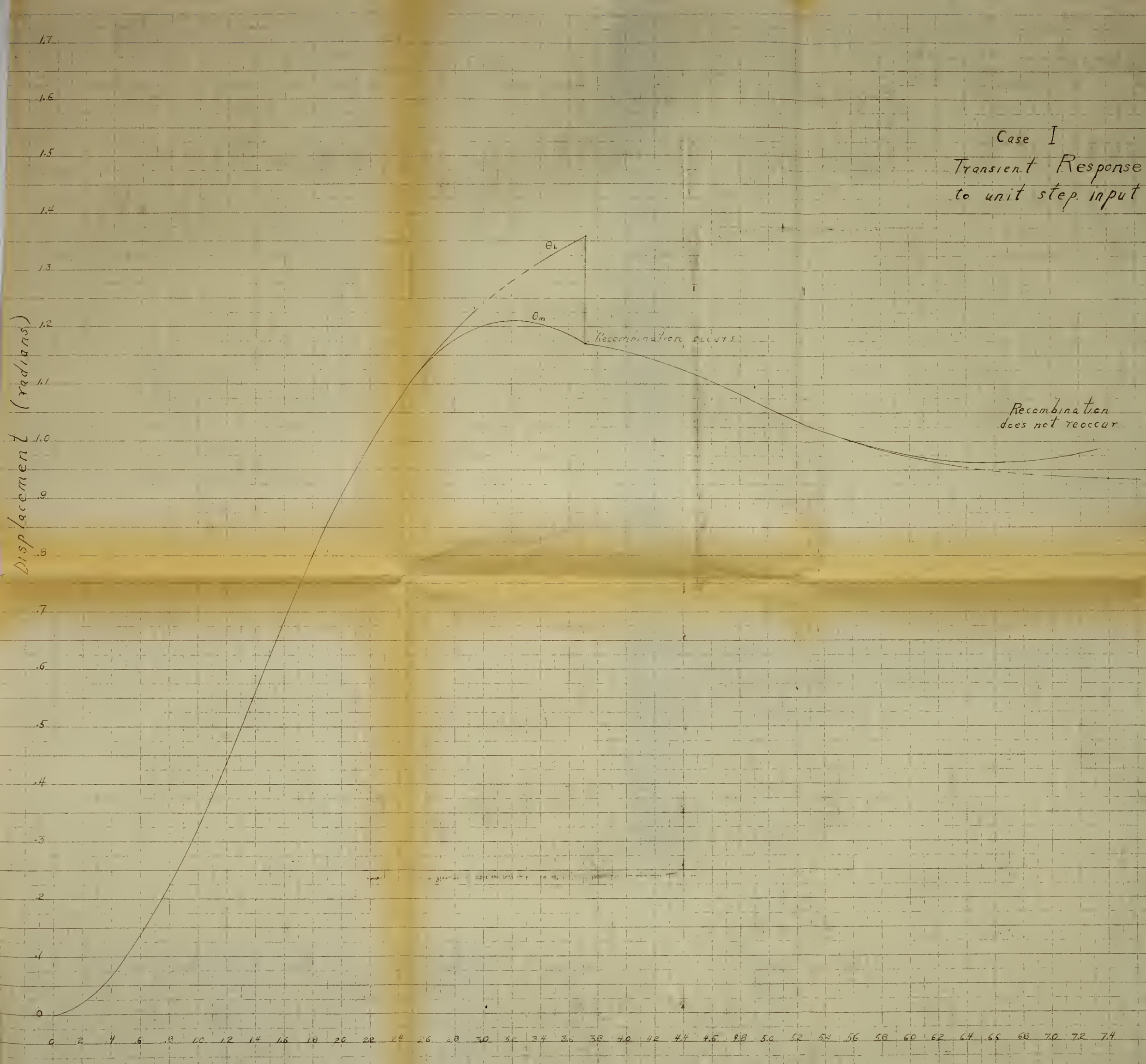

Figure 10

Case I

θ_m, θ_L
during separation

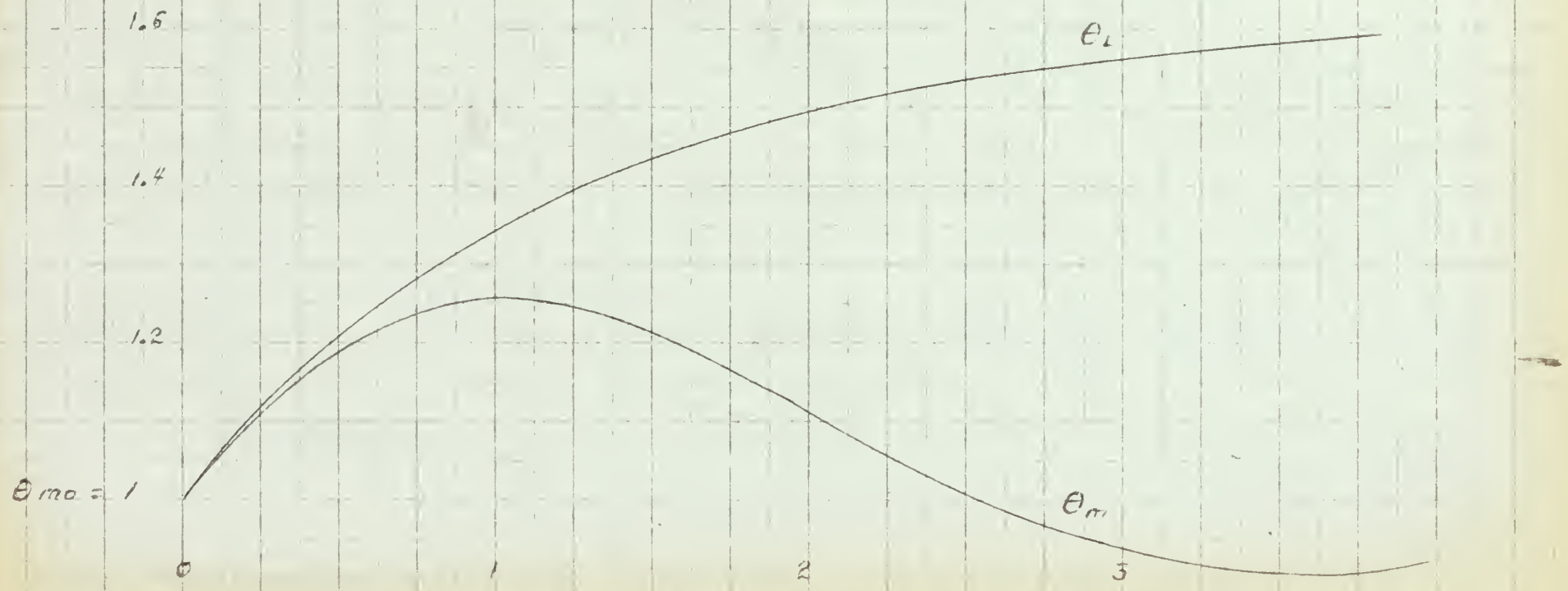

Figure 11
Page 20

Table 5

t	θ_o	θ_m	θ_L	t	θ_m	θ_L
.258	.026			5.710	.9929	.9929
.520	.1			5.810	.986	.986
.759	.2			6.010	.9758	.9747
1.133	.4			6.210	.9681	.9648
1.472	.6			6.410	.9635	.9564
1.805	.8			6.61	.9619	.9491
2.221	1.0					
Separation occurs at $\dot{\theta}_{L_o}$ .42						
2.321		1.0393	1.0393			
2.421		1.075	1.075			
2.621		1.134	1.14			
3.021		1.202	1.242			
3.221		1.211	1.282			
3.421		1.206	1.315			
3.721		1.177	1.358			
Recombination occurs						
4.369	1.130					
4.837	1.08					
5.545	1.01					
5.61	1.00					
Separation occurs at $\dot{\theta}_{L_o}$ -.074						

From Fig.9 it may be seen that the system as described is stable and contains a residual steady state displacement error $\leqslant$ the amount of the backlash. A step displacement input of 1.0 is seen to separate

into load and system without load at $\theta_c = 1$, $\dot{\theta}_{L0} = .42$, at point A. The load is seen to follow a constant deceleration isocline of -.8 while the system without the load converges towards the stable focus. Recombination occurs when the system without load is at B and the load is at B′ . The momentum balance causes the recombined trajectory to originate from point C. Separation reoccurs at point D and recombination does not occur thereafter since the output measuring device is inside the limits of the backlash. The load comes to rest with -.091 rad. residual error.

A step displacement input originating at $\theta_0 = 1$, $\dot{\theta}_c = 1$ is seen to separate at $\theta_0 = 1$, recombine when the system without load is at E and the load is at E′ . The recombined trajectory is seen to originate from F, reseparate at G, recombine at H, H′ , I and separate again at J where the output detector is once again inside the backlash region so that further correction is impossible.

Fig. 10 describes the transient response to a step displacement input of 1.0 rad. From the figure it may be seen that system resonant frequency changes between combined and uncombined systems, and that velocity changes abruptly upon recombination.

Fig. 11 is a plot of θ_m, θ_L at separation.

7. Case II. Output measured at motor shaft.

Load possesses no viscous friction.

Given system.

Combined

(56) $1\ddot{\theta}_o + .2\dot{\theta}_o + \theta_o = 1$

System as closed loop with load separated.

(57) $.5\ddot{\theta}_m + .2\dot{\theta}_m + \theta_m = 1$

Load separately

(58) $.5\ddot{\theta}_L = 0$

Backlash .3 rad.

Isocline at which load separates from system is determined by the isocline equation for the load.

(58) $.5\ddot{\theta}_L + 0\dot{\theta}_L = 0 \qquad \eta_3 = 0$

To find the isoclines for the combined system, letting $\theta_R = 1$

(59) $\eta_1 + .2 = \dfrac{1 - \theta_o}{\dot{\theta}_o}$

Slopes of the isoclines are given in Table six.

Table 6

η_1	$\arctan \frac{\dot{\theta}_o}{1-\theta_o}$	η_1	$\arctan \frac{\dot{\theta}_o}{1-\theta_o}$	η_1	$\arctan \frac{\dot{\theta}_o}{1-\theta_o}$
∞	0°	.2	-68.2°	-3	19.66°
10	- 5.61°	.1	-73.3°	-5	11.77°
7	- 7.91°	0	-78.7°	-7	8.36°
5	-10.9°	-.1	-84.3°	-10	5.83°
3	-17.35°	-.2	-90°		
2.5	-20.35°	-.3	84.3°		
2.0	-24.5°	-.5	73.3°		
1.5	-30.45°	-.7	63.4°		
1.2	-35.55°	-1.0	51.35°		
1.0	-39.8°	-1.2	45°		
.7	-48°	-1.5	37.6°		
.5	-55°	-2.0	29.05°		
.3	-63.4°	-2.5	23.5°		

To find isoclines for the system with load separated

(60) $$\eta_2 + .4 = 2\left(\frac{1 - \theta_m}{\dot{\theta}_m}\right)$$

Slopes of the isoclines are given in Table seven.

Table 7

η_2	$\arctan \frac{\dot\theta_m}{1-\theta_m}$	η_2	$\arctan \frac{\dot\theta_m}{1-\theta_m}$
∞	0	- .1	-81.46°
10	-10.89°	- .2	-84.3°
7	-15.3°	- .3	-87.15°
5	-20.33°	- .4	-90°
3	-30.45°	- .5	87.15°
2.5	-34.6°	- .7	81.46°
2.0	-39.8°	-1.0	73.3°
1.5	-46.45°	-1.2	68.2°
1.2	-51.3°	-1.5	61.2°
1.0	-55.0°	-2.0	51.3°
.7	-61.2°	-2.5	43.6°
.5	-65.75°	-3.0	37.6°
.3	-70.7°	-5.0	23.5°
.2	-73.3°	-7.0	17.39°
.1	-75.9°	-1.0	11.78°
0	-78.7°		

To obtain dividing lines for $\theta_m \dot\theta_m$, $\theta_L \dot\theta_L$, $\theta_o \dot\theta_o$ at recombination,

(57) $$\ddot\theta_m + .4\,\dot\theta_m + 2\theta_m = 2$$

In LaPlace form

(61) $$\theta_m = \frac{2/s + \dot\theta_{mo} + s\theta_{mo} + .4\theta_{mo}}{(s^2 + .4s + 2)}$$

Roots of quadratic factor are $-.2 \pm j\,1.4$

(62) $$\theta_m = 1 + .715\,\dot\theta_{mo}\, e^{-.2t} \sin(1.4t - \phi)$$

where $\phi = 16.25°$

(63) $\dot{\theta}_m = -.1430\ \dot{\theta}_{mo}\, e^{-.2t} \sin(1.4t - \phi) + \dot{\theta}_{mo}\, e^{-.2t} \cos(1.4t - \phi)$

For load separately

(64) $\theta_L = \frac{\dot{\theta}_{Lo}}{s^2} + \frac{\theta_{Lo}}{s}$

(65) $\theta_L = \dot{\theta}_{Lo}\, t + \theta_{Lo}$

Substituting values of (t) in factors of equation (62) results in values of Table eight.

Table 8

t	$\sin(1.4t-\phi)$	$e^{-.2t}$	t	$\sin(1.4t-\phi)$	$e^{-.2t}$
0	-.284	1	10.0	.917	.1358
.2	-.008	.9608	11.0	.581	.111
.4	.258	.9231	12.0	-.725	.091
.6	.524	.887	13.0	-.824	.0743
.8	.739	.852	14.0	.430	.061
1.0	.895	.819	15.0	.972	.050
1.2	.983	.7865	16.0	-.070	.041
1.4	.999	.756	17.0	-.997	.0335
1.6	.928	.726	18.0	-.250	.0274
1.8	.790	.698	19.0	.906	.0225
2.0	.588	.670	20.0	.523	.0184
3.0	-.693	.549			
4.0	-.824	.449			
5.0	.415	.386			
6.0	.968	.301			
7.0	-.078	.247			
8.0	-.995	.202			
9.0	-.276	.166			

When the terms of Table eight are plotted in accordance with equations (62) and (65), for $\dot{\theta}_{mo}=1$ figure 12 is obtained.

From figure twelve, the times of recombination for .3 rad. backlash are determined for various values of $\dot{\theta}_{mo}$ as described in section 3, thus describing dividing lines for $\theta_m \dot{\theta}_m$, $\theta_L \dot{\theta}_L$, $\theta_o \dot{\theta}_o$ at recombination. Values determined are as listed in Table nine. Values of $\theta_m \dot{\theta}_m$, $\theta_L \dot{\theta}_L$ were determined from equations (62), (63) and (65). $\dot{\theta}_o$ values were determined from equation (24).

Table 9

t	$\dot{\theta}_{mo}$	θ_m	$\dot{\theta}_m$	$\dot{\theta}_o$
1.36	.5	.272	-.07125	.21437
1.40	.45	.242	-.0828	.1839
1.49	.40	.2075	-.1082	.1459
1.56	.35	.1745	-.1157	.1171
1.66	.30	.136	-.1236	.0882
1.82	.25	.0970	-.1297	.0602
2.0	.20	.0560	-.11946	.0402
2.3	.15	.0135	-.0953	.0273
2.63	.12	-.0127	-.0663	.0268
2.95	.10	-.025	-.047	.0265
3.22	.09	-.02975	-.0167	.0366
3.63	.08	-.0275	.0088	.0444
3.95	.075	-.01215	.03283	.0534
4.40	.07	-.00253	.0292	.0364
4.95	.065	.0050	.0217	.0434
5.45	.06	.0126	.00726	.0310
6.36	.05	.0075	-.0111	.0195
7.56	.04	-.00487	-.00464	.0178
8.47	.035	-.00383	.00438	.01969
10.08	.03	.00249	.00184	.0159
12.0	.025	-.00118	-.001327	.01183
15.1	.02	.00064	-.000519	.0102

The transient response as determined from the phase plans is tabulated in Table ten.:

Table 10

For step displacement input of .16

t	θ_o	θ_m	t	θ_o	θ_m	t	θ_m
0	0		3.1		.226	7.35	.150
.15	.0015		3.3		.214	7.55	.1485
.277	.0053		3.5		.1985	7.75	.148
.417	.0123		3.7		.1815	7.95	.1492
			System recombines				
.583	.024		3.8	.161		8.15	.1494
.762	.040		3.9	.160		8.35	.1514
.998	.066		4.31	.173		8.55	.1538
1.265	.100		4.73	.18		8.75	.1566
1.500	.132		5.33	.184		8.95	.1600
System separated from load at $\dot{\theta}_{lo} = .137$			5.72	.182			
1.7		.16	6.03	.178			
1.9		.1833	6.36	.172			
2.1		.2055	6.55	.168			
			System separates at $\dot{\theta}_{lo} = .022$				
2.3		.2217	6.75		.16		
2.5		.2817	6.95		.156		
2.7		.2356	7.15		.1527		
2.9		.2335					

Figure thirteen is a phase plane portrait of the system when it is subjected to a step in put of .1^{r} rad. The dividing lines are shown to have particularly unusual configurations for this system characterized by no viscous friction in the load, and slight damping. The θ_m $\dot{\theta}_m$ dividing line is seen to spiral into the stable focus much like a trajectory. The θ_o $\dot{\theta}_o$ dividing line for recombination is seen to consist

of a series of loops, the tops of which represent maximum energy fed back from the load upon recombination, and the bottoms of which represent minimum energy fed back. This phenomenon is attributable to the existence of a natural period for separation which permits recombination velocities to add vectorially, increasing the displacement of the system immediately after recombination.

The phase trajectory is seen to separate load from system at point A. Recombination occurs at point B, and the new θ_o $\dot{\theta}_o$ is seen to take place at C, a point of relatively low energy feedback. The system separates again at D and recombines again when θ_m is at E. The θ_o $\dot{\theta}_o$ for this recombination occurs at F, again a relatively low energy feedback, and from this convergence, it is seen that θ_o $\dot{\theta}_o$ loops approach the stable focus, making the system ultimately stable. As in case I, the output error of the system will be the magnitude of the backlash.

Figure fourteen pictures the system behavior in response to a step input of .09f. From this it may be seen that the θ_o $\dot{\theta}_o$ position upon recombination is at the top of the first loop, representing a maximum feed-back of energy from the load. The load separates from the system at A, recombines at B to produce a θ_o $\dot{\theta}_o$ for the recombined system at C. The system separates again at D and recombines when θ_m is at E, resulting in a recombined $\theta_o \dot{\theta}_o$ at F. As before, it may be seen that the system is ultimately stable, however it takes the system a longer period to settle from a step of .09f than from a step of .1f.

Figure fifteen shows the system transient performance to a step of .1f and .09f. Once again, this illustrates the more oscillatory performance induced in the system by the smaller input, when conditions are favorable for load momentum reinforcement upon recombination.

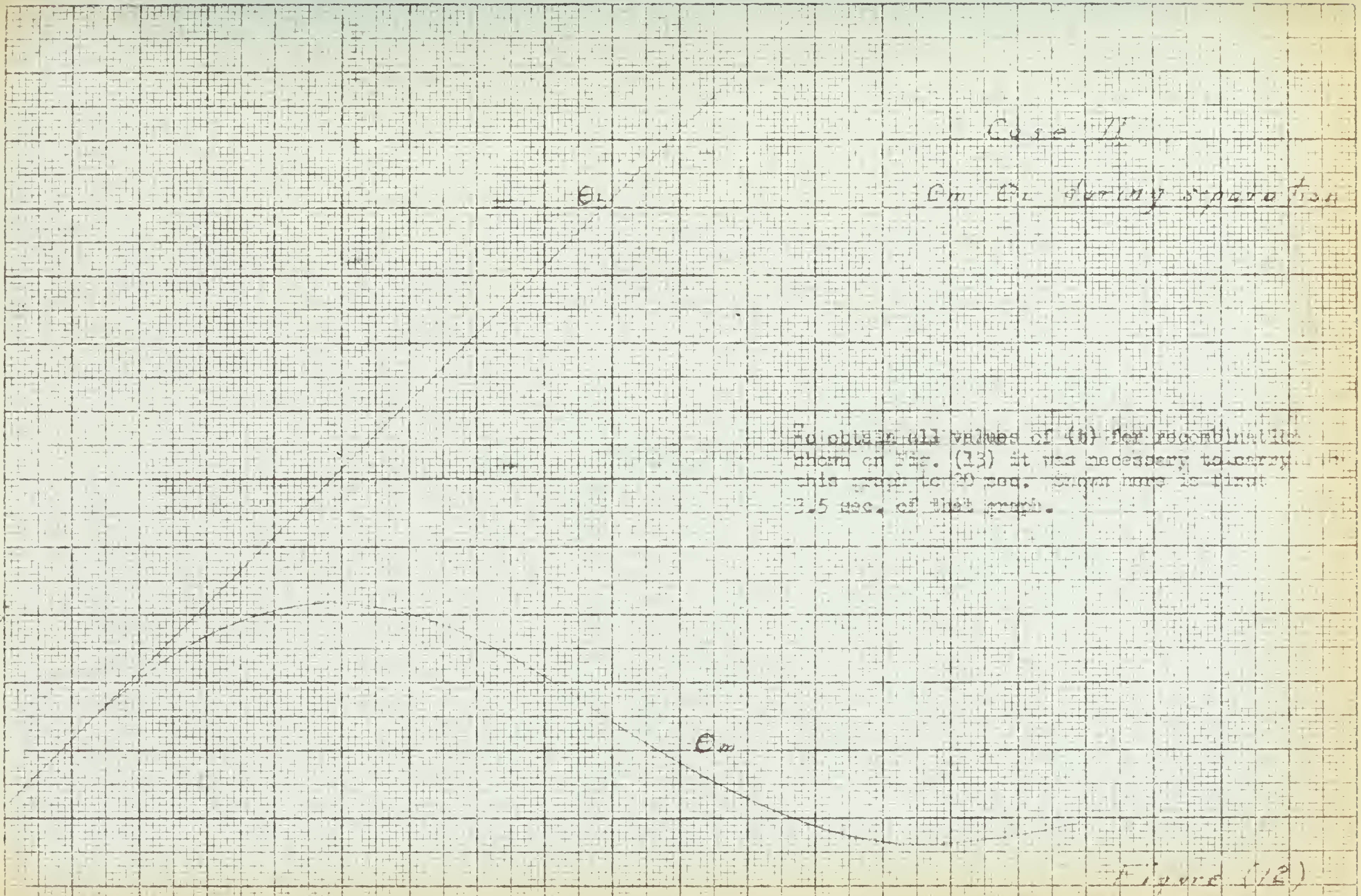
Case IV
θ_m θ_L during separation
θ_L
θ_m
3
2.5
2
1.5
1
ϵ_{mo}
.5
1
1.5
2
2.5
3
3.5
To obtain all values of (θ) for recombination shown on Fig. (13) it was necessary to carry this graph to 30 sec. Shown here is first 3.5 sec. of that graph.
Figure (12)

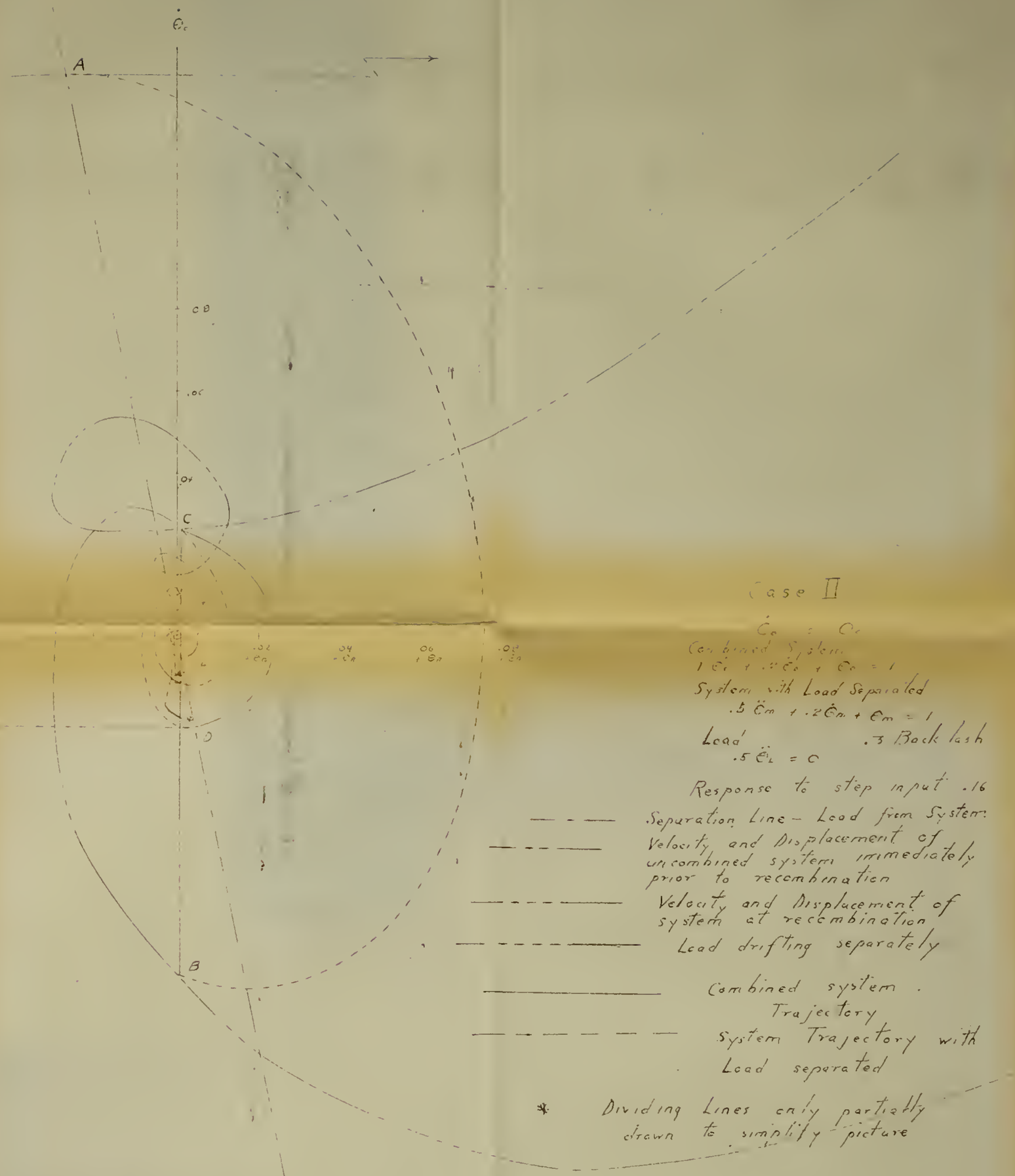
$\dot{e}_c$
A
CB
.06
.04
C
D
B
Case II
$\dot{e}_c = e_c$
Combined System
$1\ddot{e}_c + .2\dot{e}_c + e_c = 1$
System with Load Separated
$.5\ddot{e}_m + .2\dot{e}_m + e_m = 1$
Load .3 Back lash
$.5\ddot{e}_L = 0$
Response to step input .16
Separation Line – Load from System
Velocity and Displacement of uncombined system immediately prior to recombination
Velocity and Displacement of system at recombination
Load drifting separately
Combined system Trajectory
System Trajectory with Load separated
* Dividing Lines only partially drawn to simplify picture

Figure 13

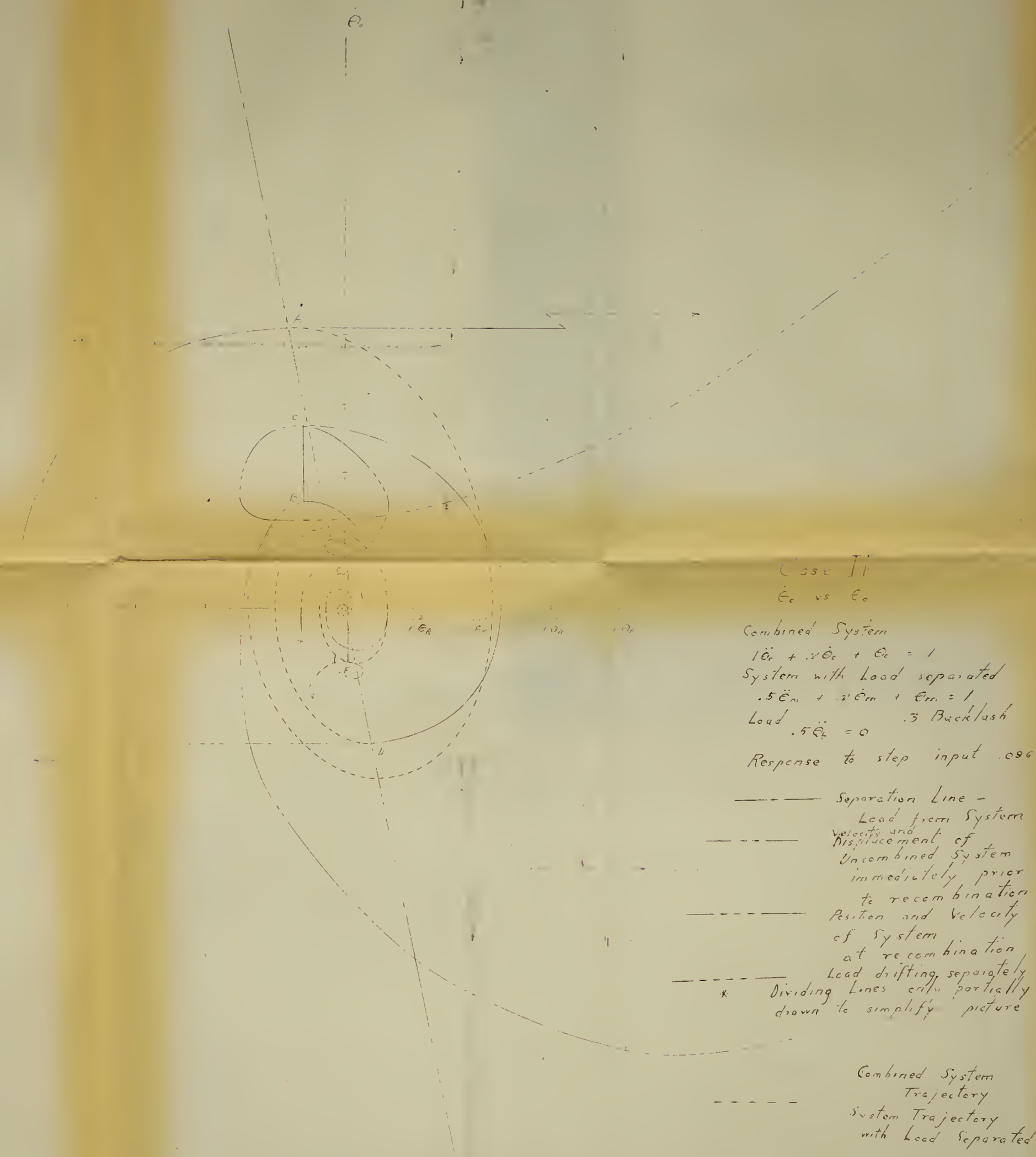
$\dot{e}_o$ vs e_o
Combined System
$1\ddot{e}_o + .2\dot{e}_o + e_o = 1$
System with Load separated
$.5\ddot{e}_m + .2\dot{e}_m + e_m = 1$
Load .3 Backlash
$.5\ddot{e}_L = 0$
Response to step input .096
Separation Line – Lead from System
Velocity and Displacement of Uncombined System immediately prior to recombination
Position and Velocity of System at recombination
Lead drifting separately
* Dividing Lines only partially drawn to simplify picture
Combined System Trajectory
System Trajectory with Lead Separated

Figure 14

Displacement (rad)

Case III. Output measured at load.

Load possesses no viscous friction. Inertia distribution is equalized between load and system without load.

Given system .3 Backlash

Combined.

(66) $1\ \ddot{\theta}_o + .2\dot{\theta}_o + \theta_o = 1$

System as open loop with load separated.

(67) $.5\ \ddot{\theta}_m + .2\dot{\theta}_m = 1 - \theta_L$

Load separately

(68) $.5\ \ddot{\theta}_L = 0$

Slopes for the isoclines of the combined system are as tabulated in Table six. Equation (40) and (41) are applicable to system when operating in the backlash region, and reduce to

(69) $$\theta_m = \frac{13.5\ \dot{\theta}_{mo}}{s^2} - \frac{5\dot{\theta}_{mo}}{s^3} - 31.25\ \dot{\theta}_{mo}\left(\frac{1}{s} + \frac{1}{s+.4}\right) + \frac{1 - .2\ \dot{\theta}_{mo}}{s}$$

(70) $$\theta_m = 13.5\ \dot{\theta}_{mo}\ t - 2.5\ \dot{\theta}_{mo}\ t^2 - 31.25\left(\dot{\theta}_{mo}\right)\left(1 - e^{-.4t}\right) + 1 - .2\ \dot{\theta}_{mo}$$

(71) $$\dot{\theta}_m = \frac{13.5\ \dot{\theta}_{mo}}{s} - \frac{5\dot{\theta}_{mo}}{s^2} + \frac{31.25\ s\ \dot{\theta}_{mo}}{(s+.4)}$$

(72) $$\dot{\theta}_m = 13.5\ \dot{\theta}_{mo}\left(1 - e^{-.4t}\right) + \dot{\theta}_{mo}\ e^{-.4t} - 5\dot{\theta}_{mo}\ t$$

(73) $$\theta_L = \dot{\theta}_{Lo}\ t + \theta_{Lo}$$

Substituting values of (t) in factors of equations (70) and (73) results in data tabulated in Table eleven.

Table 11

t	$e^{-.4t}$	$(1-e^{-.4t})$	$-2.5t^2$	$13.5t$	$-3125(1-e^{-.4t})$	$-.2$	θ_{m-1}	$13.5(1-e^{-.4t})$	$-5t$	$\dot{\theta}_m$
0	1	0	0	0	0	-.2	-.2	0	0	1
.2	.923	.077	- .1	2.7	-2.405	-.2	-.005	1.04	-1	.[illegible]3
.4	.852	.148	- .4	5.4	-4.625	-.2	.175	2	-2	. [illegible]
.6	.7865	.2135	- .9	8.1	-6.675	-.2	..325	2.[illegible]8	-3	.[illegible]
.8	.726	.274	-1.6	10.79	-8.56	-.2	.44	3.7	-4	. [illegible]
1.0	.670	.330	-2.5	13.5	-10.32	-.2	.48	4.45	-5	.1[illegible]
1.2	.619	.381	-3.6	16.2	-11.9	-.2	.50	5.15	-6	-.231
1.4	.571	.429	-4.9	18.9	-13.4	-.2	.40	5.80	-7	-.[illegible]
1.6	.528	.472	-6.4	21.6	-14.75	-.2	.25	6.37	-8	-1.[illegible]
1.8	.487	.513	-8.1	24.29	-16.05	-.2	-.06	6.92	-9	-1.[illegible]
2.0	.450	.550	-10	27	-17.2	-.2	-.4	7.43	-10	-2.1[illegible]
2.2	.415	.585	-12.1	29.7	-18.3	-.2	-.9	7.9	-11	- .[illegible]
2.4	.383	.617	-14.4	32.4	-19.3	-.2	-1.5	8.33	-12	-3.[illegible]
2.6	.354	.646	-16.9	35.1	-20.2	-.2	-2.2	8.73	-13	-3.[illegible]
2.8	.326	.674	-19.6	37.8	-21.03	-.2	-3.03	9.1	-14	-4.[illegible]
3.0	.3015	.698	-22.5	40.5	-21.8	-.2	-4.0	9.43	-15	-[illegible]
3.2	.278	.722	-25.6	43.2	-22.6	-.2	-5.2	9.75	-16	- [illegible]
3.4	.257	.743	-28.9	45.9	-23.2	-.2	-6.4	10.0	-17	-[illegible]
3.6	.2375	.7625	-32.4	48.6	-23.8	-.2	-7.8	10.3	-18	-7.[illegible]
3.8	.219	.781	-36.1	51.3	-24.[illegible]	-.2	-9.4	10.[illegible]5	-19	-[illegible]
4.0	.202	.798	-40	54.0	-24.95	-.2	-11.15	10.77	-20	-[illegible]

Figure sixteen is a graph of values tabulated in Table eleven. When scaled for various values of $\dot{\theta}_{mo}$ on the Seperation dividing lines, values of (t) are obtained as described in section 3, which are the times required for recombination to occur for a specific $\dot{\theta}_{mo}$. These values are listed with corresponding values of $\dot{\theta}_m$ in Table twelve, with factors from equations(70) and (72).

Table 12

$\dot{\theta}_{mo}$	t	$e^{-.4t}$	$(1-e^{-.4t})$	$-25t^2$	$13.5t$	$\frac{-3125}{(1-e^{-.4t})}$	$-.2$	θ_m -/
1	.98	.676	.324	- 2.4	13.21	-10.12	-.2	.49
.5	1.27	.602	.398	- 4.045	17.15	-12.42	-.2	.243
.4	1.37	.578	.422	- 4.70	18.5	-13.2	-.2	.17
.3	1.52	.544	.456	- 5.77	20.52	-14.26	-.2	.087
.2	1.75	.4965	.5035	- 7.63	23.6	-15.71	-.2	.012
.1	2.25	.406	.594	-12.68	30.4	-18.55	-.2	-.103
.09	2.41	.381	.619	-14.5	32.52	-19.32	-.2	-.12
.06	2.68	.342	.658	-17.0	36.2	-20.56	-.2	-.14
.04	3.1	.290	.710	-24.0	41.9	-22.20	-.2	-.1
.02	4.0	.202	.798	-40.0	54	-24.9	-.2	-.292

Table 12 continued

$\dot{\theta}_{mo}$	t	$\frac{13.5}{(1-e^{-.4t})}$	$-5t$	$\dot{\theta}_m$
1	.98	4.375	-4.9	.151
.5	1.27	5.375	-6.35	-.1865
.4	1.37	5.7	-6.85	-.2288
.3	1.52	6.16	-7.6	-.2688
.2	1.75	6.19	-8.75	-.2927
.1	2.25	8.01	-11.25	-.2834
.08	2.41	8.35	-12.05	-.271
.06	2.68	8.88	-13.4	-.2507
.04	3.1	9.58	-15.5	-.225
.02	4.0	10.78	-20.0	- .180

From equation (24) it is determined that corresponding values of θ_o, $\dot{\theta}_o$ for recombination are as listed in Table thirteen.

Table 13

$\dot{\theta}_{mo}$	$\dot{\theta}_o$	θ_o
.1	.5755	.78
.5	.1567	.535
.4	.0858	.469
.3	.0156	.396
.2	-.0464	.310
.1	-.0918	.205
.08	-.0955	.1769
.06	-.0953	.1488
.04	-.0927	.116
.02	-.0803	.076

Figure seventeen is the phase plane plot of the system with pertinent dividing lines.

It is seen that a step displacement input of 1.145 spirals into a limit cycle with a constant amplitude of 1.030 while a step displacement of .057 diverges into the identical limit cycle.

When the system is operating in a limit cycle, separation occurs at A, recombination occurs when $\theta_m \dot{\theta}_m$ is at B and $\theta_L, \dot{\theta}_L$ is at B'. The recombined phase trajectory originates from point C on the $\theta_o \dot{\theta}_o$ dividing line and the system separates again at D.

Applying stability criteria of section 4 yields the following:

At separation, $\dot{\theta}_o = .45$, $\theta_R - \theta_o = .096$ in limit cycle.

Substituting into equation (38), C = .524

Upon recombination in limit cycle, $\dot{\theta}_o = .12$, $\theta_R - \theta_o = -.5$

Substituting into equation (38), C = .512.

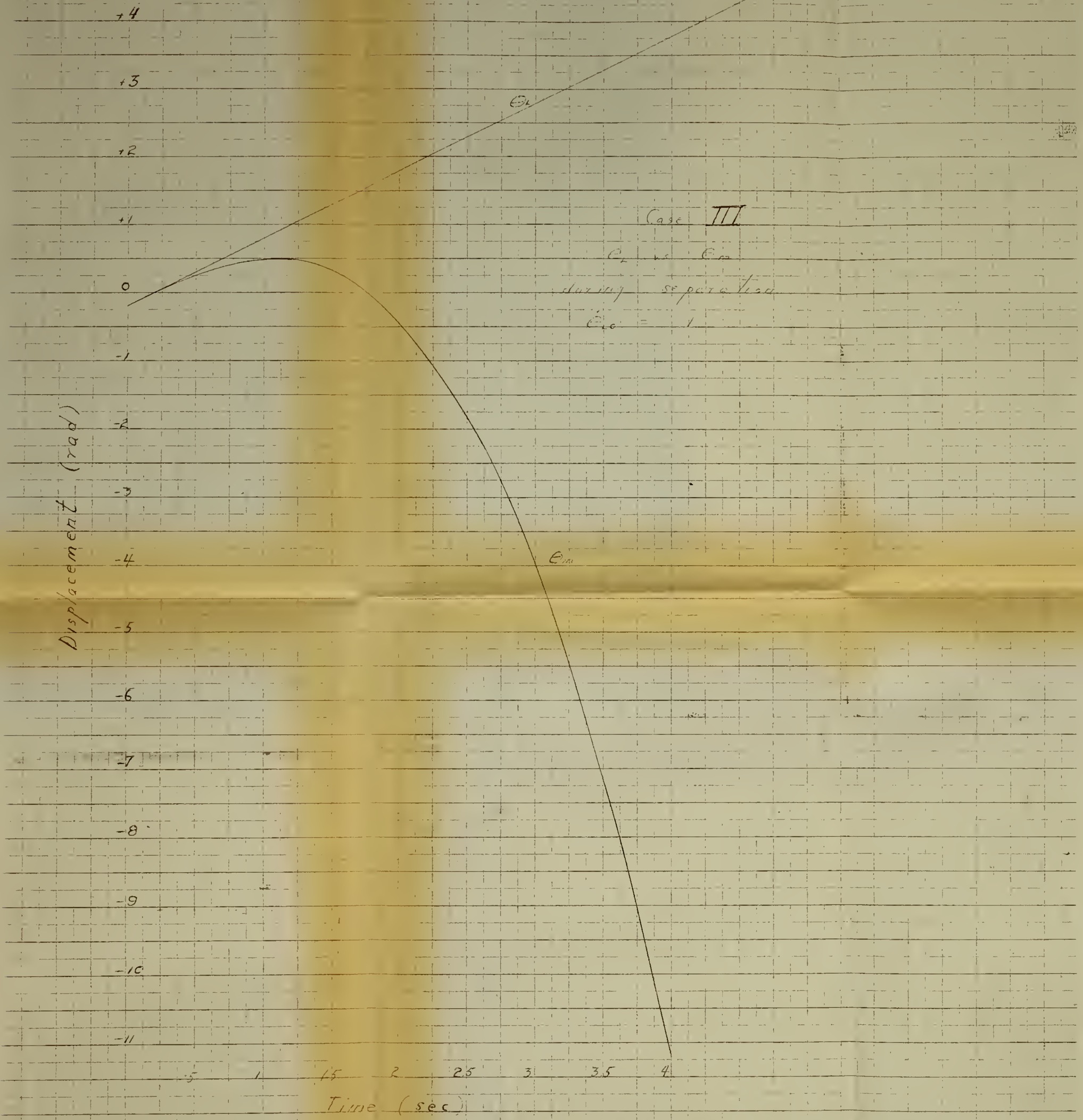
+4
+3
+2
+1
0
-1
-2
-3
-4
-5
-6
-7
-8
-9
-10
-11
Displacement (rad)
.5
1
1.5
2
2.5
3
3.5
4
Time (sec)
θ_L
θ_m
Case III
θ_L vs θ_m
during separation
$\dot{\theta}_{L0} = 1$

Figure (16)

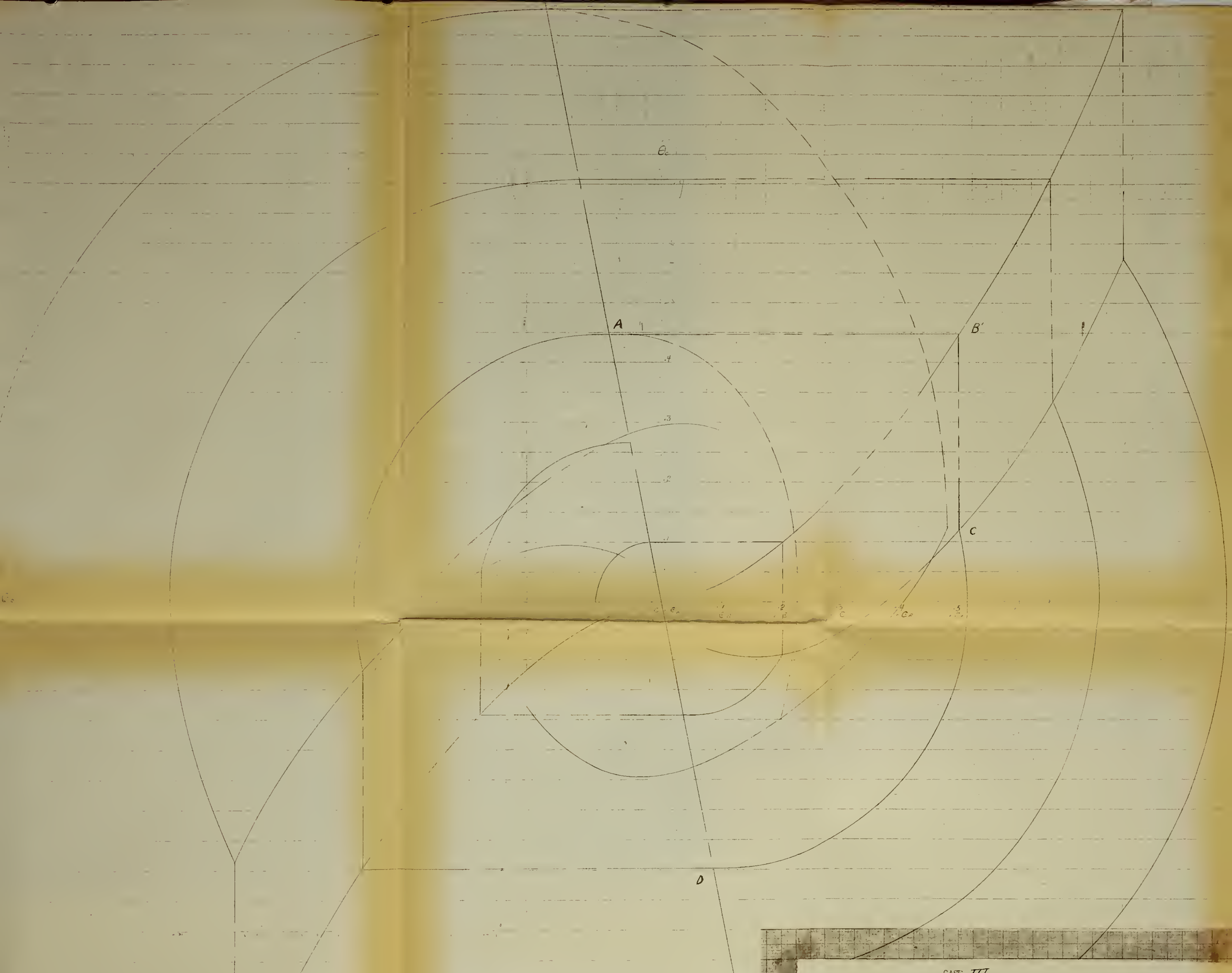

CASE III

PHASE PLANE θ_o vs $\dot{\theta}_o$ θ_L vs $\dot{\theta}_L$

COMBINED $\ddot{\theta}_o + .2\dot{\theta}_L + \theta_o = 1$

SYSTEM WITH LOAD SEPARATED $.5\ddot{\theta}_m + .2\dot{\theta}_m = 1 - \theta_L$

LOAD $.5\ddot{\theta}_L + 0\dot{\theta}_L = 0$

BACKLASH .3 RAD.

- COMBINED SYSTEM TRAJECTORY
- TRAJECTORY OF SYSTEM WITH LOAD SEPARATED
- SEPARATION DIVIDING LINE
- VELOCITY AND DISPLACEMENT OF SYSTEM WITHOUT LOAD AT RECOMBINATION
- VELOCITY AND DISPLACEMENT OF SYSTEM AT RECOMBINATION
- VELOCITY AND DISPLACEMENT OF LOAD DURING SEPARATION
- VELOCITY AND DISPLACEMENT OF LOAD AT RECOMBINATION

Figure (17)

9. Case IV. Output measured at load.

Load possesses no viscous friction and has greater part of inertia.

Given system .3 rad backlash

(74) $1\ddot{\theta}_o + .2\dot{\theta}_o + \theta_o = 1$

System as open loop with load separated

(75) $.2\ddot{\theta}_m + .2\dot{\theta}_m = 1 - \theta_L$

Load separately

(76) $.8\ddot{\theta}_L = 0$

Slopes of the isoclines of the combined system are as tabulated in Table six.

Equations (40) and (41) are applicable to system when operating in the backlash region, and reduce to

(77) $\theta_m = -2.5\dot{\theta}_{mo}t^2 + 6\dot{\theta}_{mo}t - 5\dot{\theta}_{mo}(1 - e^{-t}) + 1 - .2\dot{\theta}_{mo}$

(78) $\dot{\theta}_m = -5\dot{\theta}_{mo}t + 6\dot{\theta}_{mo} - 5\dot{\theta}_{mo}e^{-t}$

(79) $\theta_L = \dot{\theta}_{Lo}t + \theta_{Lo}$

Substituting values of (t) in factors of equations (77) and (78) results in data tabulated in Table fourteen.

Table 14

t	e^{-t}	$(1-e^{-t})$	$-25t^2$	$6t$	$(1-e^{-5t})$	$-.2$	$\theta_m - 1$
.2	.819	.181	- .1	1.2	-.995	-.2	-.005
.4	.670	.330	- .4	2.4	-1.65	-.2	.15
.6	.549	.451	- .9	3.6	-2.26	-.2	.25
1.0	.368	.632	- 2.5	6	-3.16	-.2	.14
1.2	.302	.698	- 3.6	7.2	-3.49	-.2	-.09
1.4	.247	.753	- 4.9	8.4	-3.76	-.2	-.46
1.6	.202	.798	- 6.4	9.6	-3.99	-.2	-.99
1.8	.166	.834	- 8.1	10.8	-4.16	-.2	-1.66
2.0	.136	.864	-10.0	12.0	-4.31	-.2	-2.51
2.2	.111	.889	-12.2	13.2	-4.44	-.2	-3.64
2.4	.091	.909	-14.4	14.4	-4.54	-.2	-4.74
2.6	.074	.926	-16.9	15.6	-4.63	-.2	-6.13
2.8	.061	.939	-19.6	16.8	-4.69	-.2	-7.69
3.0	.05	.950	-22.5	18.0	-4.75	-.2	-9.45
3.2	.041	.959	-25.6	19.2	-4.79	-.2	-11.39
3.4	.0335	.967	-28.9	20.4	-4.83	-.2	-13.53
3.6	.027	.973	-32.4	21.6	-4.86	-.2	-15.86
3.8	.0223	.978	-36.0	22.8	-4.89	-.2	-18.29
4.0	.0184	.982	-40	24	-4.90	-.2	-21.1

Table 14 continued

t	$-5t$	$-5e^{-t}$	$+6$	$\dot{\theta}_m$
.2	- 1	-4.095	6	.905
.4	- 2	-3.35	6	.65
.6	- 3	-2.74	6	.26
.8	- 4	-2.25	6	-.25
1.0	- 5	-1.84	6	-.84
1.2	- 6	-1.51	6	-1.51
1.4	- 7	-1.235	6	-2.235
1.6	- 8	-1.01	6	-3.01
1.8	- 9	- .83	6	-3.83
2.0	-10	- .68	6	-4.68
2.2	-11	- .555	6	-5.56
2.4	-12	- .455	6	-6.45
2.6	-13	- .342	6	-7.34
2.8	-14	- .305	6	-8.31
3.0	-15	- .250	6	-9.25
3.2	-16	- .205	6	-10.21
3.4	-17	- .1675	6	-11.17
3.6	-18	- .135	6	-12.14
3.8	-19	- .1115	6	-13.11
4.0	-20	- .092	6	-14.09

Figure eighteen is a graph of equations (77) and (79) Times of recombination are obtained from appropriate ordinate scaling of Fig. 17 for various values of $\dot{\theta}_{mo}$ as was done in Case III. Values of (t), corresponding to $\dot{\theta}_{mo}$ and factors of time solutions for equations (77) and (79) are listed in Table 15.

Table 15

$\dot{\theta}_{mo}$	t	e^{-t}	$(1-e^{-t})$	$-2.5t^2$	$6t$	$-\frac{5}{(1-e^{-t})}$	$-.2$	$\theta_m - 1$
1	.78	.459	.541	-1.525	4.675	-2.71	-.2	.240
.8	.825	.438	.562	-1.7	4.95	-2.81	-.2	.192
.6	.92	.399	.601	-2.115	5.51	-3.005	-.2	.111
.4	1.06	.346	.654	-2.8	6.35	-3.265	-.2	.034
.2	1.36	.257	.743	-4.61	8.15	-3.715	-.2	-.075
.1	1.75	.174	.826	-7.65	10.5	-4.135	-.2	-.135
.08	1.90	.150	.850	-9.0	11.4	-4.25	-.2	-.150
.06	2.11	.122	.878	-11.11	12.67	-4.395	-.2	-.1681
.04	2.48	.084	.916	-15.38	14.89	-4.58	-.2	-.2110
.02	3.25	.039	.961	-26.4	19.5	-4.80	-.2	-.2314

$\dot{\theta}_{mo}$	$-5t$	$5(1-e^{-t})$	$+1$	$\dot{\theta}_m$
1	- 3.9	2.71	1	-.19
.8	- 4.12	2.81	1	-.248
.6	- 4.6	3.005	1	-.357
.4	- 5.3	3.265	1	-.414
.2	- 6.8	3.715	1	-.417
.1	- 8.75	4.135	1	-.3615
.08	- 9.5	4.395	1	-.340
.06	-10.54	4.25	1	-.3087
.04	-12.4	4.58	1	-.2782
.02	-16.22	4.80	1	-.2084

From equation (24) values of θ_o, $\dot{\theta}_o$ are listed in Table sixteen for recombination

Table 16

$\dot{\theta}_{mo}$	θ_o	$\dot{\theta}_o$
1	.78	.762
.8	.68	.5904
.6	.552	.4086
.4	.424	.2372
.2	.272	.0766
.1	.175	.0077
.08	.15	-.004
.06	.1266	-.01374
.04	.0992	-.02364
.02	.0650	-.02568

Figure nineteen is the phase plane portrait of the system. The magnitude of the limit cycle in this case is 1.150 which considering the difference in inertia distribution between cases III and IV, is not appreciably greater than the 1.030 magnitude of case III.

A step displacement input of .69 is seen to spiral into the limit cycle while a step of .435 is seen to spiral out toward the same limit cycle.

When the system is performing a limit cycle, it is seen to separate at A. The backlash of .3 rad. is not taken up until the system with load removed has reached B and the load has reached B'. Recombination occurs and the recombined trajectory originates from C. Separation reoccurs on the separation dividing line of point D.

Applying the stability criteria of section 4 to the limit cycle of case IV yields the following.

For equation (38), the applicable constants are

$K = 1$

$F = .2$

$J = 1$

At separation $\dot{\theta}_o = .495$

$\theta_R - \theta_o = .095$

Substituting in equation (38)

(80) $C = \sqrt{\dfrac{(.495)^2 - (.2)(.495)(.095) + (.095)^2}{1 - \frac{.2^2}{4}}}\; e^{\frac{.2/2}{\sqrt{1-.2^2/4}}\left(\frac{\arctan .495}{.095} - \frac{\pi}{2}\right)}$

$= .556$

Upon recombination,

$\dot{\theta}_o = .315$

$\theta_R - \theta_o = -.485$

Substituting in equation (38)

(81) $C = \sqrt{\dfrac{(.315)^2 - (.2)(-.485) + (-.485)^2}{1 - \frac{.2^2}{4}}}\; e^{\frac{.2/2}{\sqrt{1-\frac{.2^2}{4}}}\left(\frac{\arctan(.315)}{(-.485)} - \frac{\pi}{2}\right)}$

$= .618$, which represents only fair agreement.

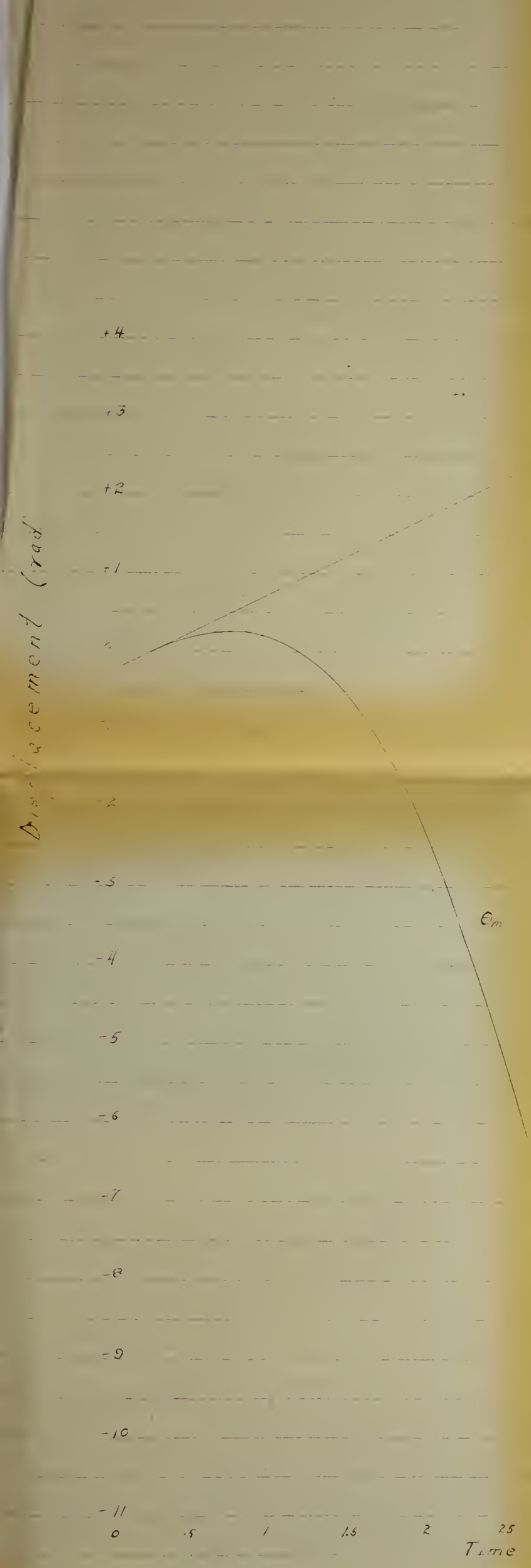

Case IV

θ_m , θ_L during separation

Figure 18

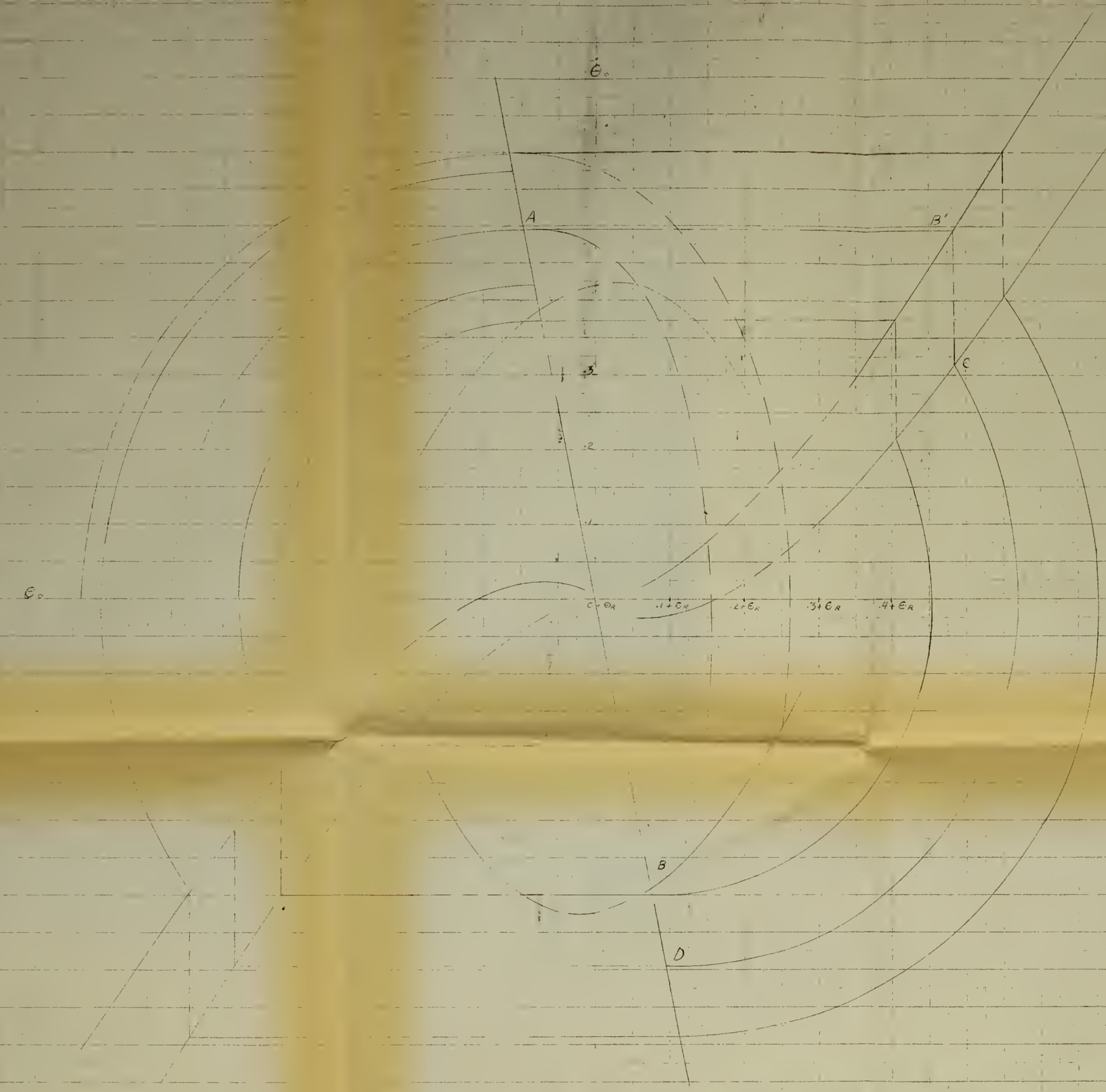

CASE IV

PHASE PLANE	θ_o vs $\dot{\theta}_o$	θ_L vs $\dot{\theta}_L$
COMBINED	$1\ \ddot{\theta}_o + .2\ \dot{\theta}_o + \theta_o = 1$	
SYSTEM WITH LOAD SEPARATED	$.2\ \ddot{\theta}_m + .2\ \dot{\theta}_m = 1 - \theta_L$	
LOAD	$.8\ \ddot{\theta}_L + 0\ \dot{\theta}_L = 0$	
BACKLASH	.3 RAD.	

COMBINED SYSTEM TRAJECTORY
TRAJECTORY OF SYSTEM WITH LOAD SEPARATED
SEPARATION DIVIDING LINE
VELOCITY AND DISPLACEMENT OF SYSTEM WITHOUT LOAD AT RECOMBINATION
VELOCITY AND DISPLACEMENT OF SYSTEM AT RECOMBINATION
VELOCITY AND DISPLACEMENT OF LOAD DURING SEPARATION
VELOCITY AND DISPLACEMENT OF LOAD AT RECOMBINATION

Figure (19)

10. Case V. Outout measured at load.

Load possesses viscous friction. Inertia equally divided between load and system with load separated.

Given system .3 rad. backlash.

$$(82)\quad \ddot{\theta}_o + .4\dot{\theta}_o + \theta_o = 1$$

System as open loop with load separated

$$(83)\quad .5\ddot{\theta}_m + .1\dot{\theta}_m = 1 - \theta_L$$

Load separately

$$(84)\quad .5\ddot{\theta}_L + .3\dot{\theta}_L = 0$$

To obtain isoclines for the combined system.

$$(85)\quad \gamma_1 + .4 = \frac{(1 - \theta_o)}{\dot{\theta}_o}$$

$$(86)\quad \theta_o = 1 - \dot{\theta}_o(N_1 + .4)$$

Computed values of arctan $\frac{\dot{\theta}_o}{1 - \theta_o}$ for various values of N_1 are as listed in Table seventeen.

Table 17

η_1	$\arctan \frac{\dot{\theta}_o}{1-\theta_o}$	η_1	$\arctan \frac{\dot{\theta}_o}{1-\theta_o}$
∞	0°	-.2	-78.7°
10	- 5.5°	-.3	-84.3°
7	- 7.7°	-.5	84.3°
5	-10.5°	-.6	78.7°
3	-16.4°	-.7	73.3°
2.5	-19°	-1	59°
2	-22.6°	-1.2	51.4°
1.5	-27.8°	-1.5	42.2°
1.2	-32°	-2	32°
1	-35.6°	-2.5	25.5°
.7	-42.3°	-3	21.1°
.5	-48°	-5	12.3°
.3	-55°	-7	8.6°
.2	-59°	-10	5.95°
.1	-63.5°		
0	-68.2°		
-.1	-73.3°		

To obtain the isocline of the system without load, where separation of the load from the system occurs, solve for $\ddot{\theta}_L/\dot{\theta}_L$

(87) $$\ddot{\theta}_L/\dot{\theta}_L = \eta_3 = -.6$$

At instant of separation,

(88) $$\frac{\ddot{\theta}_m}{\dot{\theta}_m} + .2 = \frac{2(1-\theta_L)}{\dot{\theta}_m}$$

(89) $$\eta_2 + .2 = 2\left(\frac{1-\theta_{mo}}{\dot{\theta}_m}\right)$$

(90) $$\frac{\dot{\theta}_{mo}}{1-\theta_{mo}} = \frac{2}{\eta_2 + .2}$$

Letting N2 = N3 = -.6

(91) $\arctan \frac{\dot{\theta}_{mo}}{(1-\theta_{mo})} = 78.7^\circ \qquad \phi = 78.7^\circ$

Equation (40) reduces to

(92) $$\theta_m = 1 + 126.3\,\dot{\theta}_{mo} - 140\,\dot{\theta}_{mo}\,e^{-.2t} + 13.9\,\dot{\theta}_{mo}\,e^{-.6t} - 18.66\,\dot{\theta}_{mo}\,t$$

Equation (41) reduces to

(93) $$\dot{\theta}_m = -18.66\,\dot{\theta}_{mo} + 28\,\dot{\theta}_{mo}\,e^{-.2t} - 8.33\,\dot{\theta}_{mo}\,e^{-.6t}$$

Figure 20 is a plot of θ_m θ_L during separation. Times of recombination are obtained from this plot as described in section three. Table eighteen is a tabulation of equations (92) and (93)

Table 18

t	$e^{-.2t}$	$e^{-.6t}$	$-140\ e^{-.2t}$	$139e^{-.6t}$	$-1866t$	126.3	$\theta_m - 1$
.2	.9607	.887	-134.5	12.31	- 3.74	126.3	.37
.4	.923	.787	-129	10.92	- 7.46	126.3	.76
.6	.887	.698	-124.0	9.70	-11.2	126.3	.80
.8	.852	.619	-119.1	8.60	-14.91	126.3	.89
1.0	.819	.549	-114.5	7.63	-18.66	126.3	. .77
1.2	.787	.487	-110.1	6.76	-22.4	126.3	.56
1.4	.756	.432	-105.9	6.0	-26.15	126.3	.25
1.6	.726	.383	-101.7	5.32	-29.9	126.3	.13
1.8	.698	.340	- 97.5	4.73	-33.6	126.3	- .07
2.0	.670	.302	- 93.75	4.20	-37.4	126.3	- .65
2.2	.644	.268	- 90	3.72	-41.0	126.3	- .98
2.4	.619	.237	- 86.5	3.30	-44.85	126.3	-1.75
2.6	.595	.210	- 83.3	2.92	-48.5	126.3	-2.58
2.8	.572	.186	- 80.1	2.58	-52.25	126.3	-3.17
3.0	.549	.166	- 76.9	2.305	-56.0	126.3	-4.29
3.2	.528	.147	- 73.9	2.02	-59.7	126.3	-5.38
3.4	.507	.130	- 71.0	1.81	-63.5	126.3	-6.36
3.6	.487	.116	- 68.15	1.61	-67.1	126.3	-7.34
3.8	.468	.102	- 65.5	1.42	-71.0	126.3	-8.78
4.0	.45	.091	- 63.0	1.262	-74.6	126.3	-10.04

Table 1 continued

t	$28e^{-.2t}$	$-8.33e^{-.6t}$	-18.66	$\dot{e}_m$
.2	26.93	-7.39	-18.66	.88
.4	25.8	-6.55	-18.66	.59
.6	24.85	-5.80	-18.66	.35
.8	23.82	-5.15	-18.66	.01
1.0	22.9	-4.57	-18.66	-.33
1.2	22.0	-4.05	-18.66	-.71
1.4	21.18	-3.6	-18.66	-1.08
1.6	20.33	-3.19	-18.66	-1.52
1.8	19.35	-2.83	-18.66	-1.94
2.0	18.75	-2.52	-18.66	-2.43
2.2	18.0	-2.23	-18.66	-2.89
2.4	17.3	-1.975	-18.66	-3.34
2.6	16.65	-1.75	-18.66	-3.76
2.8	16.0	-1.55	-18.66	-4.21
3.0	15.35	-1.38	-18.66	-4.69
3.2	14.79	-1.225	-18.66	-5.10
3.4	14.2	-1.083	-18.66	-5.54
3.6	13.65	- .966	-18.66	-5.98
3.8	13.10	- .850	-18.66	-6.41
4.0	12.6	- .758	-18.66	-6.82

To obtain the θ_L $\dot{\theta}_L$ dividing line, equation (22) reduces to

(94) $$\theta_L = 1 + .2\,\dot{\theta}_{mo} + 1.66\,\dot{\theta}_{mo}\left(1 - e^{-.6t}\right)$$

Values of equation (94) are tabulated in Table nineteen

Table 19

t	$e^{-.6t}$	$(1-e^{-.6t})$	$\frac{1.66}{(1-e^{-.6t})}$	.2	$\theta_L - 1$
.2	.887	.113	.1878	.2	.3878
.4	.787	.213	.354	.2	.594
.6	.698	.302	.501	.2	.701
1.0	.549	.451	.750	.2	.950
1.4	.432	.568	.943	.2	1.143
1.8	.340	.660	1.096	.2	1.296
2.2	.268	.732	1.215	.2	1.415
2.6	.210	.790	1.31	.2	1.51
3.0	.166	.834	1.385	.2	1.585
3.4	.130	.870	1.445	.2	1.645
3.8	.102	.898	1.49	.2	1.69
4.0	.091	.909	1.51	.2	1.71

Values of θ_m $\dot{\theta}_m$, θ_L $\dot{\theta}_L$ for dividing lines are listed in Table twenty.

Table 20

$\dot{\theta}_{mo}$	t	$e^{-.2t}$	$e^{-.6t}$	$-140e^{-.2t}$	$139e^{-.6t}$	$-18.66t$	126.3	$\theta_m = 1$
1	1.075	.807	.525	-112.95	7.30	-20.05	126.3	.6
.8	1.15	.7947	.502	-111.0	6.98	-21.42	126.3	.688
.6	1.275	.775	.466	-108.35	6.49	-23.79	126.3	.3895
.4	1.45	.7482	.4195	-104.65	5.82	-27.03	126.3	.176
.2	1.81	.6965	.338	- 97.5	4.70	-33.75	126.3	-.05
.1	2.35	.6255	.244	-87.5	3.39	-43.85	126.3	-.166
.08	2.55	.601	.217	-84.1	3.02	-47.5	126.3	-.182
.06	2.85	.566	.181	-79.25	2.52	-53.1	126.3	-.2116
.04	3.30	.517	.138	-72.4	1.919	-61.5	126.3	-.227
.03	3.70	.4775	.109	-66.9	1.515	-69.0	126.3	-.242

Table 20 continued

$\dot{\theta}_{mo}$	$28e^{-.2t}$	$-8.33e^{-.6t}$	-18.66	$\dot{\theta}_m$
1	22.59	-4.37	-18.66	-.44
.8	22.2	-4.18	-18.66	-.511
.6	21.65	-3.88	-18.66	-.533
.4	20.92	-3.486	-18.66	-.49
.2	19.5	-2.812	-18.66	-.384
.1	17.51	-2.03	-18.66	-.318
.08	16.81	-1.805	-18.66	-.292
.06	15.85	-1.506	-18.66	-.259
.04	14.47	-1.15	-18.66	-.2133
.03	13.35	- .909	-18.66	-.1865

Table 20 continued

$\dot{\theta}_{mc}$	t	$e^{-.5t}(1-e^{-.6t})$	$(1-e^{-.6t})^{1.66}$	$.2$	$\theta_L - 1$	$\dot{\theta}_L$
1	1.075	.525	.475	.789	.2	.989	.525
.8	1.15	.502	.498	.826	.2	.82	.401
.6	1.275	.466	.534	.886	.2	.651	.28
.4	1.45	.4195	.5805	.965	.2	.466	.1675
.2	1.81	.338	.662	1.10	.2	.26	.0676
.1	2.35	.244	.756	1.255	.2	.1455	.0244
.08	2.55	.217	.783	1.30	.2	.12	.01735
.06	2.85	.181	.819	1.36	.2	.0936	.01085
.04	3.30	.138	.862	1.43	.2	.06525	.00552
.03	3.70	.109	.891	1.48	.2	.0505	.00327

Equation (24) yields values for $\dot{\theta}_o$ upon recombination, as tabulated in Table twenty-one.

Table 21

$\dot{\theta}_{r_0}$	$\dot{\theta}_0$
1	.0425
.8	-.055
.6	-.1265
.4	-.16125
.2	-.1582
.1	-.1468
.08	-.1373
.06	-.1241
.04	-.1039
.03	-.0916

Fig. 21 is the phase plane portrait of θ_0 $\dot{\theta}_0$, θ_2 $\dot{\theta}_2$
It is seen that in response to a step input of .62, the system separates at Point A, recombines when θ_1 $\dot{\theta}_2$ is at point B, and once the momentum balance has been satisfied, θ_0 for the recombined system originates from point C, reseparating at point D. This trajectory spirals in towards a limit cycle of magnitude .52 while a step input of .23 is seen to spiral outwards into the same limit cycle described by points E, F, G and H.

Case V

θ_m θ_L during separation

$\dot{\theta}_{max} = 1$

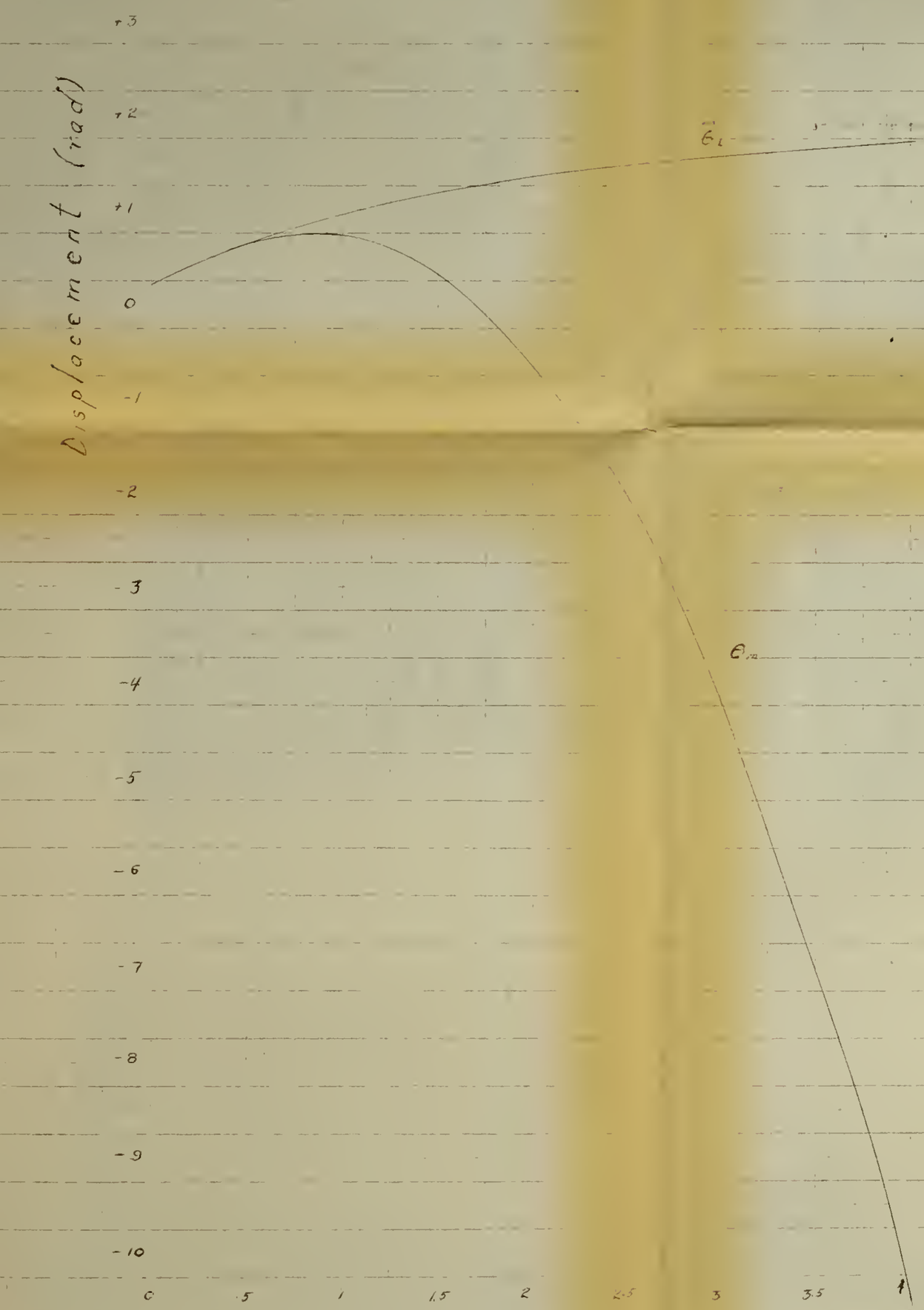

Figure 20

Page 65

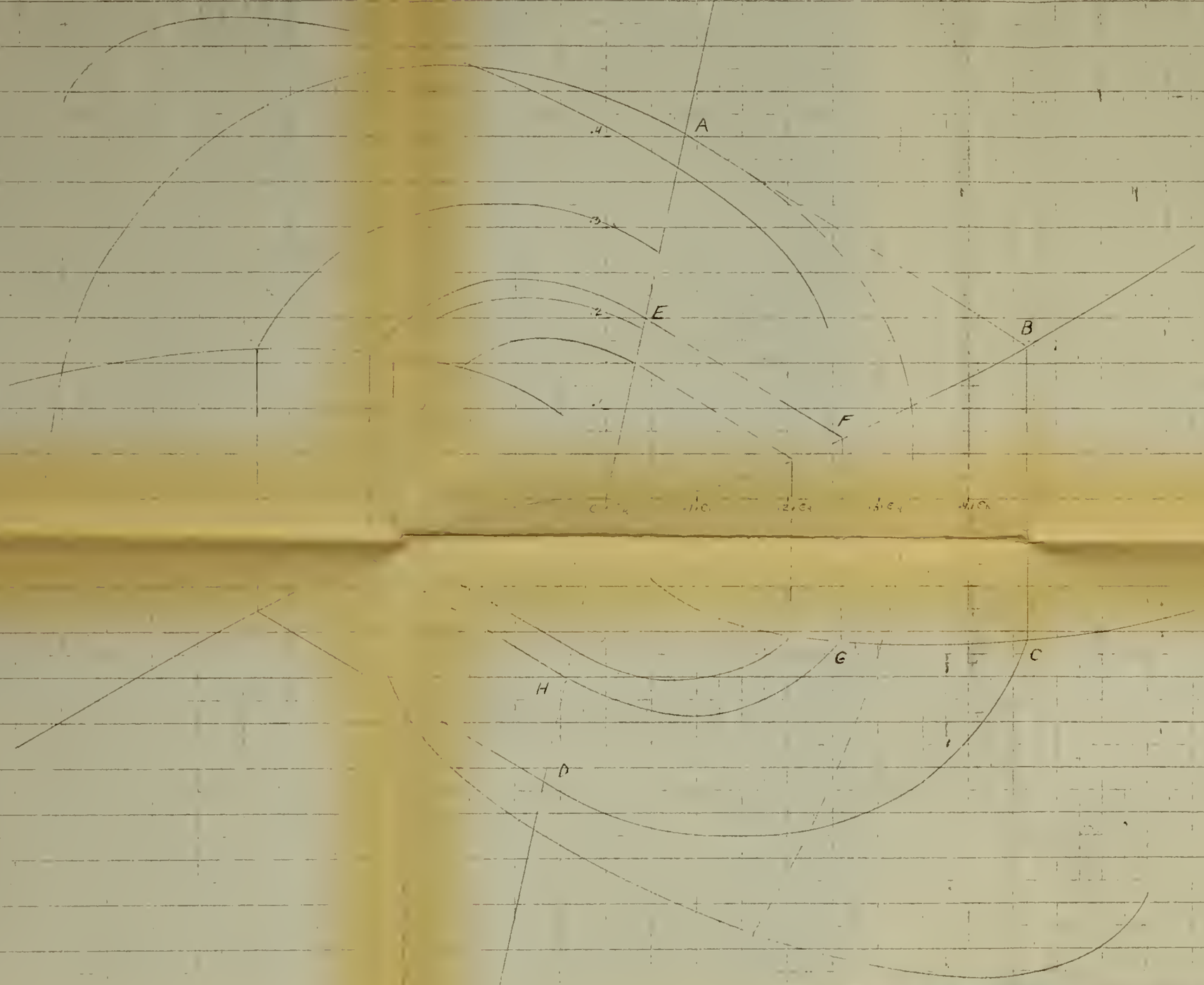

CASE V

PHASE PLANE θ_c vs $\dot{\theta}_c$ θ_L vs $\dot{\theta}_L$

COMBINED SYSTEM WITH LOAD SEPARATED
$\ddot{\theta}_c + .4\dot{\theta}_c + \theta_c = 1$
$.5\ddot{\theta}_L + .3\dot{\theta}_L = 1 - \theta_L$

LOAD $.5\ddot{\theta}_L + .3\dot{\theta}_L = 0$

BACKLASH .3 RAD.

- COMBINED SYSTEM TRAJECTORY
- TRAJECTORY OF SYSTEM WITH LOAD SEPARATED
- SEPARATION DIVIDING LINE
- VELOCITY AND DISPLACEMENT OF SYSTEM WITHOUT LOAD AT RECOMBINATION
- VELOCITY AND DISPLACEMENT OF SYSTEM AT RECOMBINATION
- VELOCITY AND DISPLACEMENT OF LOAD DURING SEPARATION
- VELOCITY AND DISPLACEMENT OF LOAD AT RECOMBINATION

Figure (21)

11. Case VI.

Output measured at load.

Load possesses viscous friction. Inertia equally divided between load and system with load separated

Given system

(95) $1\ddot{\theta}_o + .4\dot{\theta}_o + \theta_o = 1$

System as open loop with load separated. .3 rad backlash

(96) $.5\ddot{\theta}_m + .3\dot{\theta}_m = 1 - \theta_L$

Load separately

(97) $.5\ddot{\theta}_L + .1\dot{\theta}_L = 0$

Isoclines for the combined system are identical with those of case V, listed in Table seventeen.

To obtain the isocline of the system without load, where separation of the load from system occurs, solve for

(98) $\frac{\ddot{\theta}_L}{\dot{\theta}_L} = \eta_3 = -.2$

At the instant of separation

(99) $\frac{\ddot{\theta}_m}{\dot{\theta}_m} + .6 = \frac{2(1 - \theta_{mo})}{\dot{\theta}_{mo}}$

(100) $\eta_2 + .6 = \frac{2(1 - \theta_{mo})}{\dot{\theta}_{mo}}$

(101) $\frac{\dot{\theta}_{mo}}{1 - \theta_{mo}} = \frac{2}{\eta_2 + 6}$

Letting N2 = N3 = -.2

arctan $\frac{\dot{\theta}_{mo}}{1 - \theta_{mo}} = 78.7°$ $\phi = 101.3°$

Equation 40 reduces to

(102) $\theta_m = -16\dot{\theta}_{mo}t + 111.455\dot{\theta}_{mo} + 13345\dot{\theta}_{mo}e^{-.6t} - 125\dot{\theta}_{mo}e^{-.2t} + 1$

Equation 41 reduces to

(103) $\dot{\theta}_m = -16\,\dot{\theta}_{mo} - 8\,\dot{\theta}_{mo}\,e^{-.6t} + 25\,\dot{\theta}_{mo}\,e^{-.2t}$

Table twenty-two lists values of θ_m $\dot{\theta}_m$ versus (t)

Table 22

t	$e^{-.2t}$	$e^{-.6t}$	$-125\,e^{-.2t}$	$13345e^{-.6t}$	$-16t$	111.455	$\theta_m - 1$
.2	.9608	.887	-120	11.82	- 3.2	111.455	.075
.4	.923	.787	-115.15	10.5	- 6.4	111.455	.405
.6	.887	.698	-110.9	9.305	- 9.6	111.455	.260
.8	.8525	.620	-106.5	8.28	-12.8	111.455	.435
1.0	.819	.550	-102.1	7.35	-16	111.455	.70
1.2	.787	.487	- 98.25	6.50	-19.2	111.455	.505
1.4	.756	.432	-94.5	5.76	-22.4	111.455	.315
1.6	.726	.384	-90.85	5.12	-25.6	111.455	.125
1.8	.698	.340	-87.25	4.545	-28.8	111.4555	-.05
2.0	.670	.302	-83.8	4.035	-32.0	111.455	-.310
2.2	.644	.268	-80.45	3.58	-35.2	111.455	-.615
2.4	.620	.237	-77.5	3.16	-38.4	111.455	-1.285
2.6	.595	.210	-74.45	2.805	-41.6	111.455	-1.790
2.8	.572	.187	-71.5	2.50	-44.8	111.455	-2.345
3.0	.550	.166	-68.8	2.22	-48	111.455	-3.125
3.2	.528	.147	-66.0	1.961	-51.2	111.455	-3.784
3.4	.507	.130	-63.4	1.735	-54.4	111.455	-4.61
3.6	.487	.116	-60.95	1.55	-57.6	111.455	-5.545
3.8	.468	.102	-58.5	1.361	-60.8	111.455	-6.484
4.0	.450	.091	-56.2	1.213	-64	111.455	-7.532

Table 22 continued

t	$25e^{-2t}$	$-8e^{-.6t}$	-16	$\dot{\theta}_m$
.2	24	-7.1	-16	.9
.4	23.03	-6.30	-16	.73
.6	22.15	-5.575	-16	.575
.8	21.3	-4.96	-16	.34
1.0	20.42	-4.40	-16	.02
1.2	19.65	-3.895	-16	-.245
1.4	18.90	-3.455	-16	-.445
1.6	18.15	-3.065	-16	-.915
1.8	17.41	-2.72	-16	-1.31
2.0	16.73	-2.42	-16	-1.69
2.2	16.07	-2.14	-16	-2.07
2.4	15.49	-1.895	-16	-2.405
2.6	14.86	-1.68	-16	-2.82
2.8	14.30	-1.495	-16	-3.195
3.0	13.73	-1.33	-16	-3.60
3.2	13.19	-1.18	-16	-3.99
3.4	12.66	-1.04	-16	-4.38
3.6	12.16	- .929	-16	-4.769
3.8	11.69	- .816	-16	-5.126
4.0	11.22	- .728	-16	-5.508

To obtain the $\theta_L \dot{\theta}_L$ dividing line, equation (22) reduces to

$$(104)\quad \theta_L = \frac{1 - .2\,\dot{\theta}_{mo}}{5} + \frac{\dot{\theta}_{mo}}{5(s + .2)}$$

$$(105)\quad \theta_L = 1 - .2\,\dot{\theta}_{mo} + 5\,\dot{\theta}_{mo}\left(1 - e^{-.2t}\right)$$

Values of θ_L versus (t) are tabulated in Table 23

Table 23

t	$(1-e^{-.2t})$	$5(1-e^{-.2t})$	$-.2$	$\theta_L - 1$
.2	.0392	.196	-.2	.004
.4	.077	.385	-.2	.185
.6	.113	.565	-.2	.365
1.0	.181	.905	-.2	.705
1.4	.244	1.24	-.2	1.04
1.8	.302	1.52	-.2	1.32
2.2	.356	1.78	-.2	1.58
2.6	.405	2.205	-.2	1.825
3.0	.450	2.25	-.2	2.05
3.4	.493	2.465	-.2	2.265
3.8	.532	2.66	-.2	2.46
4.0	.550	2.75	-.2	2.55

Figure 22 is a graph of equations (102) and (105). By appropriate ordinate scaling as described in section three, recombination times were computed as listed in Table 24, for corresponding values of $\dot{\theta}_{mo}$ Values of $\theta_m \dot{\theta}_m \theta_L \dot{\theta}_L$ for dividing lines are listed in Table 24.

Table 24

$\dot{\theta}_{mo}$	t	$e^{-.2t}$	$e^{-.6t}$	$-125\ e^{-.2t}$	$13.345\ e^{-.6t}$	$-16\ t$	$+111.455$	$\theta_m - 1$
1	1.1	.803	.517	-100.4	6.9	-17.6	111.455	.355
.8	1.175	.791	.494	-98.9	6.6	-18.8	111.455	.298
.6	1.275	.775	.466	-96.9	6.225	-20.4	111.455	.229
.4	1.425	.752	.426	-94.0	5.7	-22.8	111.455	.142
.2	1.875	.688	.3245	-86.0	4.335	-30.0	111.455	.044
.1	2.425	.616	.234	-77.0	3.125	-38.8	111.455	-.122
.08	2.64	.590	.206	-73.8	2.75	-42.25	111.455	-.1475
.06	3.20	.528	.147	-66	1.96	-51.2	111.455	-.227
.04	3.525	.494	.1205	-61.6	1.61	-56.5	111.455	-.201
.03	3.98	.452	.092	-56.5	1.23	-63.6	111.455	-.2225

Table 24 continued

$\dot{\theta}_{mo}$	$25e^{-.2t}$	$-8e^{-.6t}$	-16	$\dot{\theta}_m$
1	20.08	-4.135	-16	-.055
.8	19.8	-3.94	-16	-.112
.6	19.35	-3.73	-16	-.222
.4	18.8	-3.41	-16	-.244
.2	17.2	-2.60	-16	-.28
.1	15.4	-1.87	-16	-.247
.08	14.75	-1.65	-16	-.232
.06	13.2	-1.175	-16	-.238
.04	12.32	-.965	-16	-.151
.03	11.3	-.735	-16	-.113

Table 24 continued

$\dot{\theta}_{mo}$	f	$\dot{\theta}_c$	$\theta_c - 1$
1	1.1	.803	.785
.8	1.175	.632	.675
.6	1.275	.465	.555
.4	1.425	.30	.4155
.2	1.875	.1375	.272
.1	2.425	.0616	.172
.08	2.64	.047	.148
.06	3.2	.0316	.1292
.04	3.525	.01975	.0933
.03	3.98	.01352	.0761

Applying equation (24) to satisfy the principle of conservation of momentum yields the following values of $\dot{\theta}_o$ upon recombination corresponding to values of $\dot{\theta}_{mo}$ upon separation, listed in Table twenty-five.

Table 25

$\dot{\theta}_{mo}$	$\dot{\theta}_o$
1	.374
.8	.260
.6	.1216
.4	.029
.2	.07125
.1	-.0927
.08	-.0925
.06	-.1032
.04	-.0656
.03	-.0497

Figure 23 is the phase plane presentation of $\theta_o, \dot{\theta}_o, \theta_L, \dot{\theta}_L$ as a combined system and when operating in the backlash region.

A step input of .55 is seen to separate the load from the system at A. Recombination takes place when the load is at B, and the balancing of momentum between the load and the system without load, causes $\theta_o, \dot{\theta}_o$ of the recombined system to originate from point C. Reseparation occurs at point D and the trajectory is seen to spiral into a limit cycle defined by points E, F, G and H.

A step input of .13 is seen to spiral outward to the same limit cycle of magnitude .550

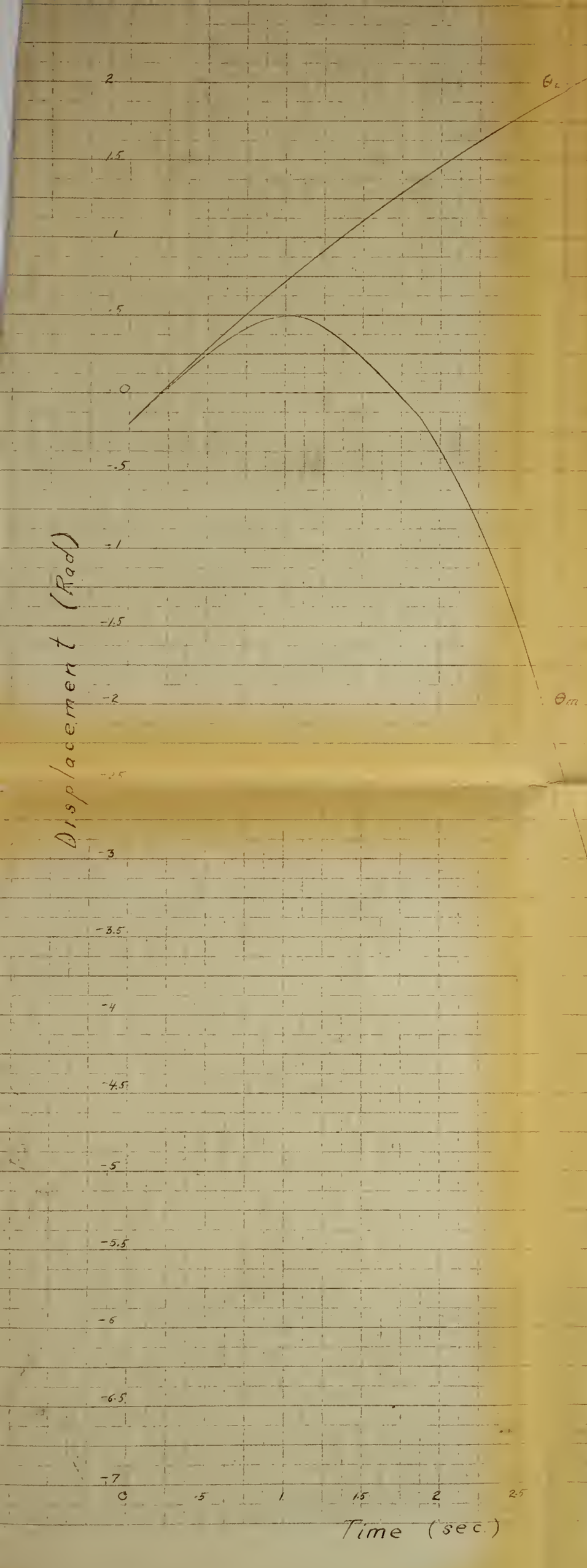

Case VI

θ_m θ_L during separation

$\dot{\theta}_{mo} = 1$

Figure 22

CASE VI

PHASE PLANE	θ_o vs $\dot{\theta}_o$	θ_L vs $\dot{\theta}_L$
COMBINED	$\ddot{\theta}_o + .4\dot{\theta}_o$	$+ \theta_o = 1$
SYSTEM WITH LOAD SEPARATED	$.5\ddot{\theta}_m +$	$.3\dot{\theta}_m = 1 - \theta_L$
LOAD	$.5\ddot{\theta}_m + .1\dot{\theta}_L = 0$	
BACKLASH	.3 RAD.	

COMBINED SYSTEM TRAJECTORY
TRAJECTORY OF SYSTEM WITH LOAD SEPARATED
SEPARATION DIVIDING LINE
VELOCITY AND DISPLACEMENT OF SYSTEM WITHOUT LOAD AT RECOMBINATION
VELOCITY AND DISPLACEMENT OF SYSTEM AT RECOMBINATION
VELOCITY AND DISPLACEMENT OF LOAD DURING SEPARATION
VELOCITY AND DISPLACEMENT OF LOAD AT RECOMBINATION

Figure (23)

12. Case VII

Output measured at load.

Load possesses viscous friction and the greater part of the system inertia.

Given system

(106) $1\ddot{\theta}_o + .4\dot{\theta}_o + \theta_o = 1$

System as open loop with load separated. .3 rad. backlash

(107) $.2\ddot{\theta}_m + .1\dot{\theta}_m = 1 - \theta_L$

Load separately

(108) $.8\ddot{\theta}_L + .3\dot{\theta}_L = 0$

Isoclines of the combined system are identical with those of case V, listed in Table seventeen.

To obtain the isocline of the system without load, where separation of the load from the system occurs, solve for

(109) $\frac{\ddot{\theta}_L}{\dot{\theta}_L} = \eta_3 = -3/8$

At the instant of separation,

(110) $\frac{\ddot{\theta}_m}{\dot{\theta}_m} + .5 = \frac{5(1 - \theta_{mo})}{\dot{\theta}_{mo}}$

(111) $\eta_2 + .5 = 5\frac{(1 - \theta_{mo})}{\dot{\theta}_{mo}}$

(112) $\frac{\dot{\theta}_{mo}}{1 - \theta_{mo}} = \frac{5}{\eta_2 + .5}$

Letting $N_2 = N_3 = -.375$

(113) $\arctan \frac{\dot{\theta}_{mo}}{1 - \theta_{mo}}$ $\arctan \frac{5}{-.375 + .5} = 88.56^\circ$ $\phi = 91.44^\circ$

Equation (40) reduces to

$$(114)\quad \theta_m = -26.4\,\dot{\theta}_{mo}\,t + 158.475\,\dot{\theta}_{mo}\,e^{-.5t} + 125.975\,\dot{\theta}_{mo} - 284.475\,\dot{\theta}_{mo}\,e^{-.375t} + 1$$

Equation (41) reduces to

$$(115)\quad \dot{\theta}_m = -26.4\,\dot{\theta}_{mo} - 79.238\,\dot{\theta}_{mo}\,e^{-.5t} + 106.638\,\dot{\theta}_{mo}\,e^{-.375t}$$

Equation 22 reduces to

$$(116)\quad \theta_L = 1 - .025\,\dot{\theta}_{mo} + 2.668\,\dot{\theta}_{mo}\left(1 - e^{-.375t}\right.$$

Equation 23 reduces to

$$(117)\quad \dot{\theta}_L = \dot{\theta}_{mo}\,e^{-.375t}$$

Table twenty-six lists values of equations (114), (115), (116) and (117) for various values of (t)

Equations (114) and (116) are plotted on Fig. 24 and various times of recombination obtained from the ordinate scaling method described in section 3.

Table 26

t	$e^{-.5t}$	$e^{-.375t}$	$158.475\,e^{-.5t}$	$-26.4t$	$-284.475\,e^{-.375t}$	$+125.975$	$\Theta_m - 1$
.2	.905	.928	143.3	- 5.28	-264	125.975	-.005
.4	.819	.861	129.8	-10.56	-245.2	125.975	.015
.6	.741	.799	117.45	-15.83	-227.3	125.975	-.295
.8	.670	.741	106.05	-21.12	-211.1	125.975	-.205
1.0	.607	.688	96.15	-26.4	-195.9	125.975	-.175
1.2	.550	.638	87.1	-31.64	-181.5	125.975	-.065
1.4	.497	.592	78.75	-37.0	-168.6	125.975	-.875
1.6	.450	.549	71.4	-42.2	-156.0	125.975	-.825
1.8	.407	.510	64.5	-47.5	-145.1	125.975	-2.125
2.0	.368	.473	58.4	-52.8	-134.7	125.975	-3.125
2.2	.333	.438	52.85	-58	-124.6	125.975	-3.775
2.4	.302	.407	47.95	-63.35	-115.85	125.975	-5.275
2.6	.272	.378	43.1	-68.55	-107.75	125.975	-7.225
2.8	.247	.350	39.2	-74.0	- 99.6	125.975	-8.425
3.0	.224	.325	35.53	-79.1	- 92.5	125.975	-10.095
3.2	.202	.302	32.0	-84.5	- 86.0	125.975	-12.525
3.4	.183	.280	29.0	-89.7	- 79.75	125.975	-14.475
3.6	.166	.260	26.3	-95.0	- 74.0	125.975	-16.725
3.8	.150	.241	23.8	-100.2	- 68.5	125.975	-18.925
4.0	.136	.224	21.54	-105.6	- 63.8	125.975	-21.885

Table 26 continued

t	$-79.238\ e^{-.5t}$	$106.638\ e^{-.375t}$	-26.4	$\dot{\theta}_m$
.2	-71.65	98.95	-26.4	.90
.4	-64.9	91.9	-26.4	.60
.6	-58.68	85.1	-26.4	.02
.8	-53.05	79.0	-26.4	-.45
1.0	-48.05	73.4	-26.4	-1.05
1.2	-43.53	68.0	-26.4	-1.93
1.4	-39.4	63.1	-26.4	-2.7
1.6	-35.62	58.5	-26.4	-3.52
1.8	-32.2	54.45	-26.4	-4.15
2.0	-29.18	50.49	-26.4	-5.09
2.2	-26.4	46.65	-26.4	-6.15
2.4	-23.93	43.40	-26.4	-6.93
2.6	-21.56	40.35	-26.4	-7.61
2.8	-19.58	37.35	-26.4	-8.63
3.0	-17.76	34.62	-26.4	-9.54
3.2	-16.0	32.2	-26.4	-10.2
3.4	-14.5	29.9	-26.4	-11.1
3.6	-13.16	27.7	-26.4	-11.86
3.8	-11.9	25.7	-26.4	-12.6
4.0	-10.79	23.9	-26.4	-13.29

Table 26 continued

t	$(1-e^{-.375t})(1-e^{-.375t})^{2.668} - .025$		$\theta_L - 1$	$\dot{\theta}_L$
.2	.072	.192	-.025	.167	.028
.4	.139	.371	-.025	.346	.861
.6	.201	.536	-.025	.511	.799
.8	.259	.6905	-.025	.6655	.741
1.0	.312	.8325	-.025	.8075	.688
1.2	.342	.9125	-.025	.8875	.638
1.4	.408	1.09	-.025	1.065	.592
1.6	.451	1.205	-.025	1.180	.549
1.8	.490	1.31	-.025	1.285	.510
2.0	.527	1.41	-.025	1.385	.473
2.2	.542	1.449	-.025	1.424	.438
2.4	.593	1.582	-.025	1.557	.407
2.6	.622	1.66	-.025	1.635	.378
2.8	.650	1.735	-.025	1.710	.350
3.0	.675	1.80	-.025	1.775	.325
3.2	.698	1.862	-.025	1.837	.302
3.4	.720	1.92	-.025	1.895	.280
3.6	.740	1.975	-.025	1.950	.260
3.8	.759	2.022	-.025	1.997	.241
4.0	.776	2.075	-.025	2.050	.224

Values of $\theta_m \dot{\theta}_m, \theta_L \dot{\theta}_L$ for recombination dividing lines are listed in table twenty-seven, for values of (t) obtained from fig. 24.

Table 27

$\dot{\theta}_{mo}$	t	$e^{-.5t}$	$e^{-.375t}$	$158.475\ e^{-.5t}$	$-26.4t$	$-284.475\ e^{-.375t}$	125.975	$\dot{\theta}_m = 1$
1	.525	.7695	.8217	121.95	-13.86	-234.0	125.975	.065
.8	.587	.746	.803	118.25	-15.5	-228.3	125.975	.340
.6	.687	.7096	.7733	112.3	-18.12	-220	125.975	.093
.4	.862	.650	.724	103.0	-22.79	-206.0	125.975	.274
.2	1.25	.536	.626	85.0	-33.0	178.3	125.975	-.[illegible]
.1	1.70	.428	.529	67.85	-44.9	-150.4	125.975	-.1475
.08	1.875	.392	.496	62.1	-49.5	-141.2	125.975	-.[illegible]
.06	2.115	.348	.453	55.15	-55.85	-129.6	125.975	-.[illegible]
.04	2.465	.292	.397	46.35	-65.05	-113.0	125.975	-.[illegible]
.02	3.275	.195	.294	30.93	-86.5	-83.75	125.975	-.2664

Table 27 continued

$\dot{\theta}_{mo}$	$-79.238\ e^{-.5t}$	$106.638\ e^{-.375t}$	-26.4	$\dot{\theta}_m$
1	-60.97	87.51	-26.4	.14
.8	-59.08	85.55	-26.4	.056
.6	-56.1	82.5	-26.4	0
.4	-51.5	77.20	-26.4	-.38
.2	-42.5	66.8	-26.4	-.42
.1	-33.88	56.45	-26.4	-.383
.08	-31.05	52.95	-26.4	-.36
.06	-27.6	48.3	-26.4	-.342
.04	-23.15	42.33	-26.4	-.289
.02	-15.48	31.3	-26.4	-.2113

Table 27 continued

$\dot{\theta}_{mo}$	t	$(1-e^{-.375t})$	$\frac{2.663}{(1-e^{-.375t})} - .025$	$\theta_L - 1$	$\dot{\theta}_L$
1	.525	.1783	.4753	-.025	.4503	.8217
.8	.587	.197	.525	-.025	.400	.6425
.6	.687	.2267	.605	-.025	.348	.464
.4	.862	.276	.736	-.025	.2842	.2993
.2	1.25	.374	.996	-.025	.1942	.1252
.1	1.70	.471	1.259	-.025	.1234	.0529
.08	1.875	.504	1.343	-.025	.1053	.0397
.06	2.115	.547	1.46	-.025	.086	.0272
.04	2.465	.603	1.61	-.025	.0635	.01589
.02	3.275	.706	1.885	-.025	.0372	.00589

Equation 24 yields values for $\dot{\theta}_o$ recombination line as follows:

Table 28

$\dot{\theta}_{mo}$	$\dot{\theta}_o$
1	.685
.2	.5252
.6	.371
.4	.1553
.2	.0161
.1	-.03425
.08	-.0402
.06	-.04629
.04	-.0451
.02	-.03755

Figure 25 is the phase plane portrait of $\theta_2 \dot{\theta}_2$ $\theta_2 \dot{\theta}_2$ for the combined and separated system. A step input of .58 is seen to separate load from system at point A. The system recombines when the load has decelerated to point B, and satisfaction of the momentum balance again causes θ_0 $\dot{\theta}_0$ to originate from point C. Reseparation occurs at point D and the trajectory is seen to converge to the limit cycle described by points E, F, G and H. A step input of .09 is seen to spiral outward to the same limit cycle of magnitude .259.

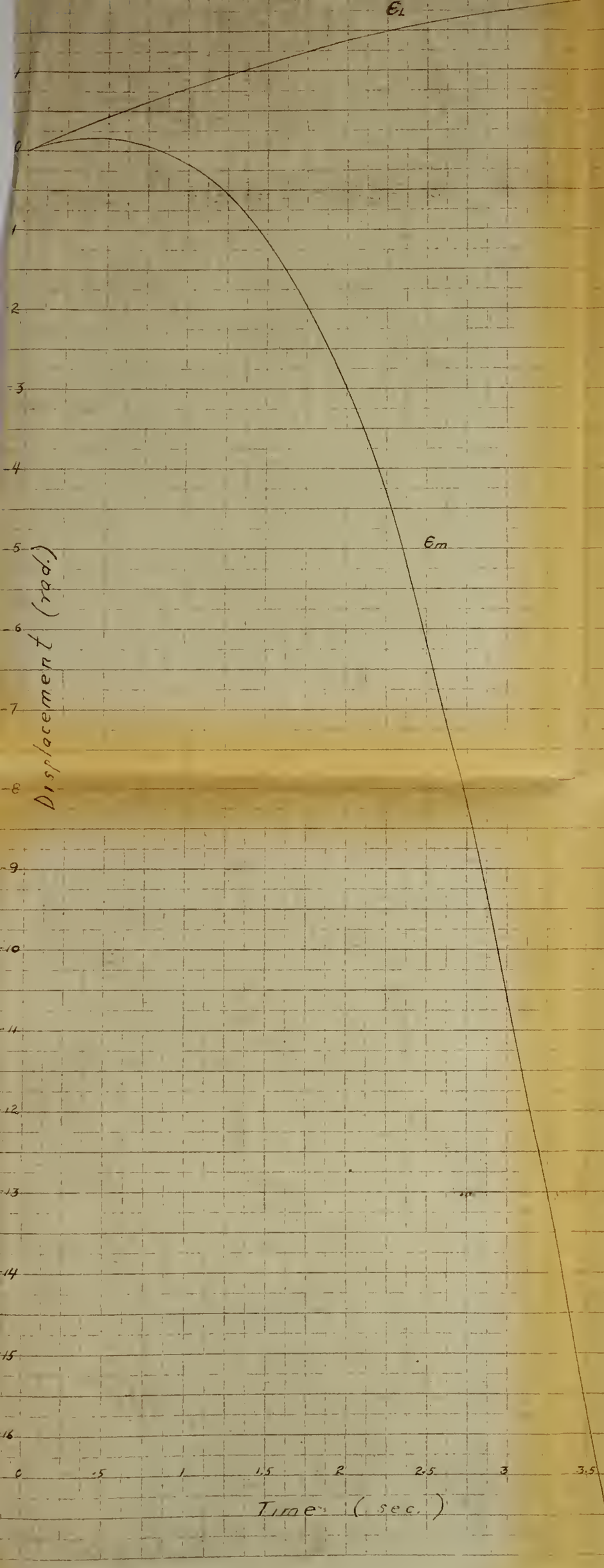

Case VII

θ_m θ_L during separation

$\dot{\theta}_{mc} = 1$

Figure 24

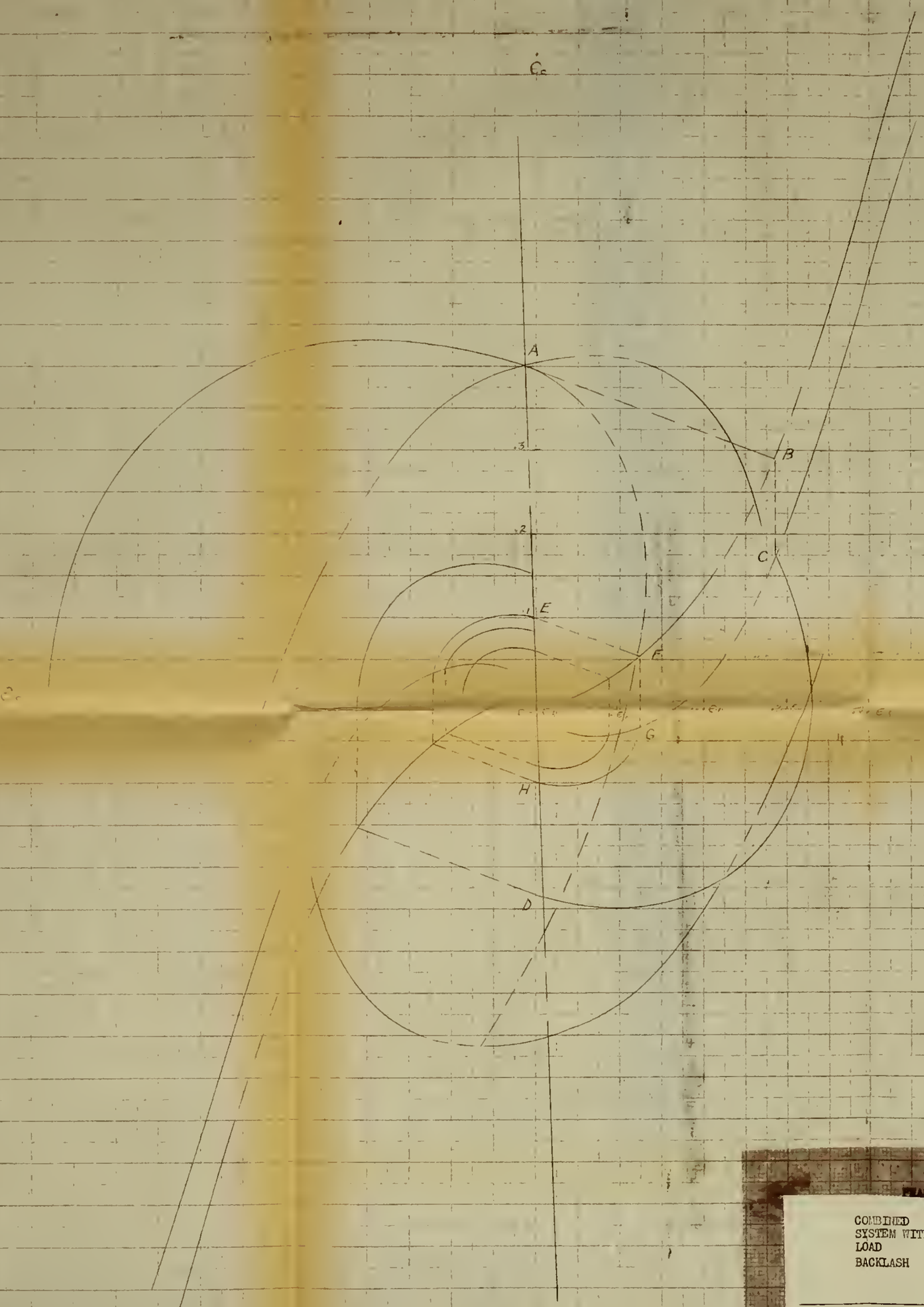

CASE VII

PHASE PLANE $\dot{e}_o$ vs $\dot{e}_o$ θ_L vs $\dot{\theta}_L$

COMBINED $1\ \ddot{\theta}_o + .4\ \dot{\theta}_o + \theta_o = 1$
SYSTEM WITH LOAD SEPARATED $.2\ \ddot{\theta}_m + .1\ \dot{\theta}_m = 1 - \theta_L$
LOAD $.8\ \ddot{\theta}_L + .3\ \dot{\theta}_L = 0$
BACKLASH .8 RAD.

COMBINED SYSTEM TRAJECTORY
TRAJECTORY OF SYSTEM WITH LOAD SEPARATED
SEPARATION DIVIDING LINE
VELOCITY AND DISPLACEMENT OF SYSTEM WITHOUT LOAD AT RECOMBINATION
VELOCITY AND DISPLACEMENT OF SYSTEM AT RECOMBINATION
VELOCITY AND DISPLACEMENT OF LOAD DURING SEPARATION
VELOCITY AND DISPLACEMENT OF LOAD AT RECOMBINATION

Figure (25)

13. Case VIII

Output measured at load

Load possesses greater part of systems inertia but lesser part of system friction.

Given system.

(118) $1\ddot{\theta}_o + .4\dot{\theta}_o + \theta_o = 1$

System as open loop with load separated. .3 rad. backlash

(119) $.2\ddot{\theta}_m + .3\dot{\theta}_m = 1 - \theta_L$

Load separately

(120) $.8\ddot{\theta}_L + .1\dot{\theta}_L = 0$

Isoclines of the combined system are identical with those of case V, listed in Table seventeen.

To obtain the isocline of the system without load, where separation of the load from the system occurs, solve for

(121) $\frac{\ddot{\theta}_L}{\dot{\theta}_L} = \eta_3 = -1/8$

At the instant of separation

(122) $\frac{\ddot{\theta}_m}{\dot{\theta}_m} + 1.5 = \frac{5(1-\theta_{mo})}{\dot{\theta}_{mo}}$

(123) $\eta_2 + 1.5 = \frac{5(1-\theta_{mo})}{\dot{\theta}_{mo}}$

(124) $\frac{\dot{\theta}_{mo}}{1-\theta_{mo}} = \frac{5}{\eta_2 + 1.5}$

Letting $N_2 = N_3 = -.125$

(125) $\arctan \frac{\dot{\theta}_{mo}}{1-\theta_{mo}} = \arctan \frac{5}{1.375} = 74.6^\circ \quad \phi = 105.4^\circ$

Equation (40) reduces to

(126) $\theta_m = -25.75\,\dot{\theta}_{mo}\,t + 231.581\,\dot{\theta}_{mo} + 1 - .125t + 1.564\,\dot{\theta}_{mo}\,e^{-1.5t} - 233.42\,e$

Equation (41) reduces to

$$(127)\quad \dot{\theta}_m = -2.34\,\dot{\theta}_{mo}\,e^{-1.5t} + 29.08\,\dot{\theta}_{mo}\,e^{-.125t} - 25.74\,\dot{\theta}_{mo}$$

Equation (22) reduces to

$$(128)\quad \theta_L = 1 - .275\,\dot{\theta}_{mo} + 8\,\dot{\theta}_{mo}\left(1 - e^{-.125t}\right)$$

Equation (23) reduces to

$$(129)\quad \dot{\theta}_L = \dot{\theta}_{mo}\,e^{-.125t}$$

Table twenty-nine is a tabulation of values of equations (126),(128), and (129) for various values of (t).

Figure (26) is a graph of equations (126) and (128). Suitable scaling of the ordinate yields recombination times for various values of $\dot{\theta}_{mo}$ as listed in Table thirty.

Equation (24) yields values of $\dot{\theta}_o$ upon recombination, as listed in Table thirty-one.

Table 29

t	$e^{-1.5t}$	$e^{-.125t}$	$1.564e^{-.5t}$	231.581	$-233.42\ e^{-.125t}$	$-25.74t$	$\Theta_m - 1$
.2	.741	.9753	1.157	231.581	-228	- 5.15	- .412
.4	.549	.951	.858	231.581	-222	-10.3	.139
.6	.407	.9278	.636	231.581	-216.1	-15.43	.687
.8	.302	.905	.4725	231.581	-211.3	-20.6	.1535
1.0	.222	.883	.3475	231.581	-206.0	-25.74	.1885
1.2	.166	.861	.260	231.581	-201.2	-30.86	-.219
1.4	.1225	.84	.192	231.581	-196.0	-36.0	-.227
1.6	.091	.819	.1422	231.581	-191.0	-41.15	-.427
1.8	.067	.7987	.105	231.581	-186.2	-46.3	-.914
2.0	.05	.779	.0783	231.581	-181.6	-51.5	-1.44
2.2	.037	.760	.058	231.581	-177.2	-56.55	-2.11
2.4	.0273	.741	.0427	231.581	-173	-61.75	-3.13
2.6	.0203	.7227	.0318	231.581	-168.6	-67.0	-3.687
2.8	.015	.705	.02345	231.581	-164.6	-72.0	-5.0
3.0	.011	.688	.0172	231.581	-160.3	-77.25	-5.952
3.2	.0091	.670	.01422	231.581	-156.3	-82.4	-7.105
3.4	.0061	.654	.00955	231.581	-152.6	-87.5	-8.510
3.6	.0045	.638	.00705	231.581	-149.0	-92.6	-10.012
3.8	.0034	.622	.005325	231.581	-145.1	-97.8	-11.314
4.0	.0025	.607	.00392	231.581	-141.5	-103	-12.915

Table 29 continued

t	$(1-e^{-.125t})$	$8(1-e^{-.125t})$	$-.275$	$\theta_L - 1$	$\dot{\theta}_L$
.2	.0247	.1978	-.275	-.0772	.9753
.4	.049	.392	-.275	.117	.951
.6	.0722	.5775	-.275	.3025	.9278
.8	.095	.76	-.275	.485	.905
1.0	.117	.936	-.275	.661	.883
1.2	.139	1.112	-.275	.837	.861
1.4	.160	1.28	-.275	1.005	.84
1.6	.181	1.45	-.275	1.175	.819
1.8	.2013	1.61	-.275	1.335	.7987
2.0	.221	1.77	-.275	1.495	.779
2.2	.240	1.92	-.275	1.645	.760
2.4	.259	2.075	-.275	1.800	.741
2.6	.2773	2.22	-.275	1.945	.7227
2.8	.295	2.36	-.275	2.085	.705
3.0	.312	2.50	-.275	2.225	.688
3.2	.330	2.64	-.275	2.365	.670
3.4	.346	2.77	-.275	2.495	.654
3.6	.362	2.898	-.275	2.623	.638
3.8	.378	3.021	-.275	2.746	.622
4.0	.393	3.14	-.275	2.865	.607

Table 30

$\dot{\theta}_{mo}$	t	$e^{-1.5t}$	$e^{-.125t}$	$1.564\ e^{-1.5t}$	231.581	$-233.42\ e^{-.125t}$	$-25.74t$	$\theta_m - 1$
1	.80	.302	.905	.4725	231.581	-211.3	-20.6	.1535
.8	.875	.270	.8964	.4215	231.581	-209.2	-22.5	.250
.6	.975	.232	.8853	.363	231.581	-206.4	-25.1	.266
.4	1.163	.175	.865	.274	231.581	-202.0	-29.96	-.042
.2	1.55	.098	.824	.1531	231.581	-192.1	-39.9	-.0532
.1	2.025	.048	.7765	.075	231.581	181.2	-52.1	-.1644
.08	2.2	.037	.760	.0579	231.581	-177.4	-56.55	-.185
.06	2.43	.026	.738	.0406	231.581	-172.1	-62.5	-.17[illegible]
.04	2.862	.0136	.6995	.02125	231.581	-163.1	-73.6	-.204
.02	3.90	.0029	.614	.00454	231.581	-143.2	-100.4	-.2405

Table 30 continued

$\dot{\theta}_{mo}$	$2.34\ e^{-1.5t}$	$29.1\ e^{-.125t}$	-25.74	$\dot{\theta}_m$
1	-.706	26.35	-25.74	-.096
.8	-.631	26.1	-25.74	-.2066
.6	-.543	25.8	-25.74	-.290
.4	-.41	25.2	-25.74	-.38
.2	-.229	24.0	-25.74	-.394
.1	-.1123	22.6	-25.74	-.325
.08	-.0865	22.13	-25.74	-.2958
.06	-.06085	21.46	-25.74	-.2602
.04	-.0318	20.35	-25.74	-.217
.02	-.00679	17.85	-25.74	-.1579

Table 30 continued

$\dot{\theta}_{mo}$	t	$(1-e^{-.125t})$	$8(1-e^{-.125t})-.275$	θ_L-1	$\dot{\theta}_L$
1	.80	.095	.76	-.275	.485	.905
.8	.875	.1036	.83	-.275	.454	.7175
.6	.975	.1147	.916	-.275	.3855	.532
.4	1.163	.135	1.08	-.275	.322	.346
.2	1.55	.176	1.41	-.275	.227	.1649
.1	2.025	.2235	1.79	-.275	.1515	.0777
.08	2.2	.240	1.92	-.275	.1316	.06075
.06	2.43	.262	2.098	-.275	.1095	.0442
.04	2.862	.3005	2.44	-.275	.0866	.028
.2	3.90	.386	3.087	-.275	.0562	.01227

Table 31

$\dot{\theta}_{mo}$	$\dot{\theta}_o$
1	.3688
.8	.3217
.6	.250
.4	.182
.2	.1027
.1	.0561
.08	.0459
.06	.0356
.04	.0259
.02	.0134

Figure 27 is the phase portrait of $\theta_o \dot{\theta}_o, \theta_L \dot{\theta}_L$ combined and separated.

A step input of .265 is seen to separate the load from the system at point A. A recombination occurs when the load has drifted to point B. $\theta_o \dot{\theta}_o$ for the recombined system originate from point C. Reseparation occurs at point D and the trajectory is seen to converge toward the limit cycle described by E, F, G, H. A step of .28 is seen to diverge toward the same limit cycle of magnitude .466.

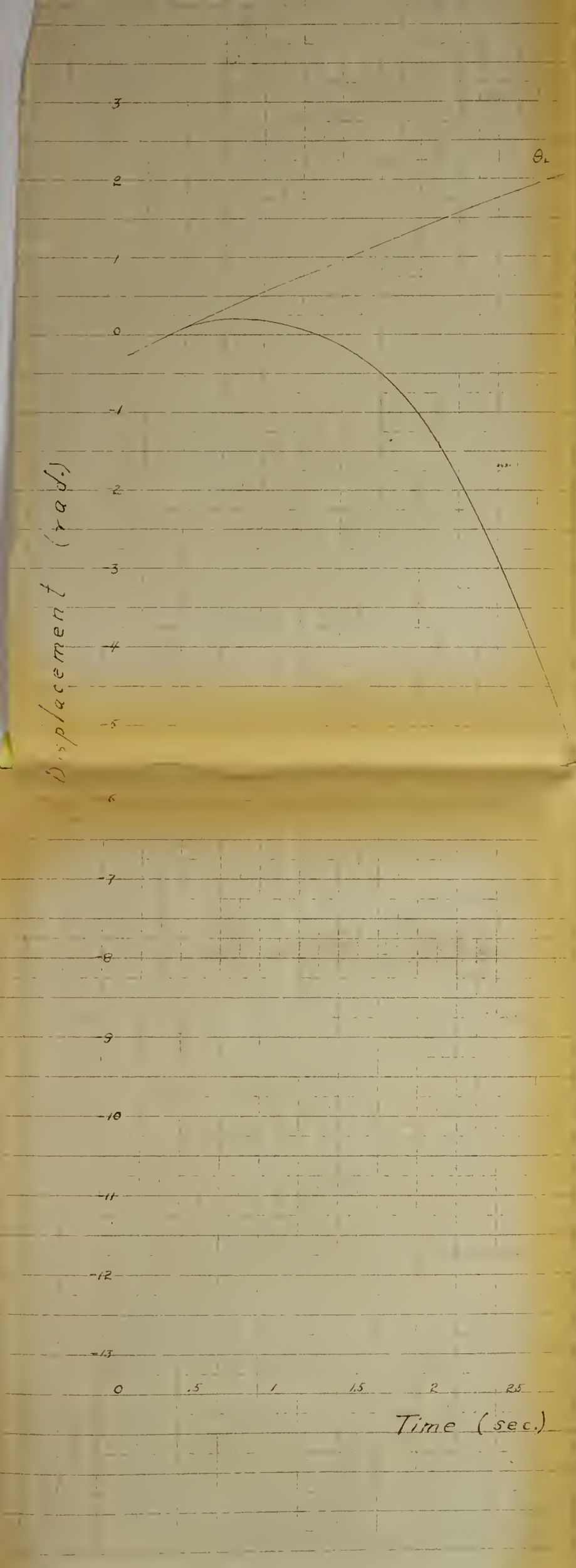

Case VII

θ_m θ_L during separation

$\dot{\theta}_{m_0} = 1$

Figure 26

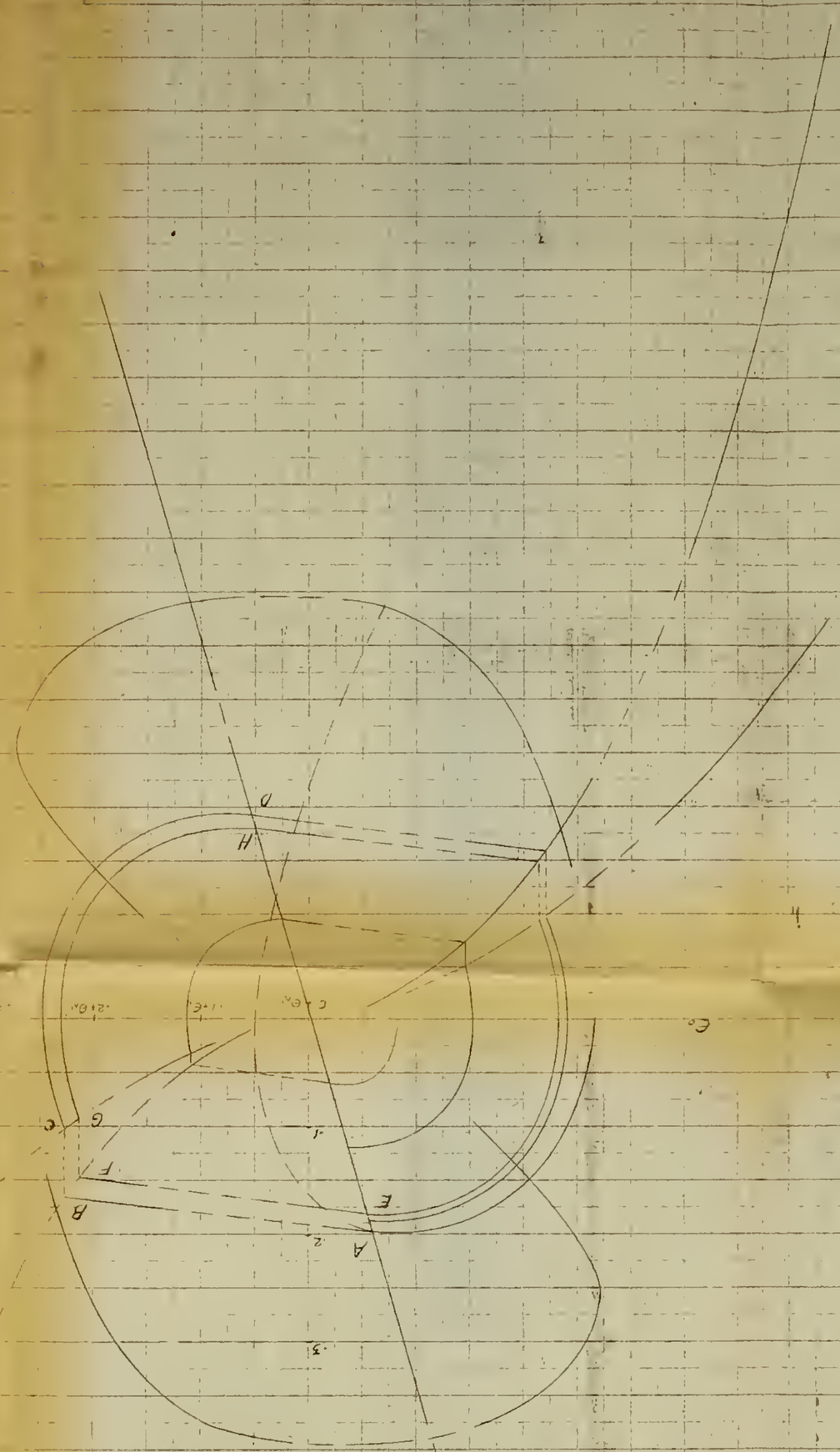

CASE VIII

PHASE PLANE θ_o vs $\dot{\theta}_o$ θ_L vs $\dot{\theta}_L$

COMBINED / $\ddot{\theta}_o + .4\,\dot{\theta}_o + \theta_o = 1$

SYSTEM WITH LOAD SEPARATED $.2\ddot{\theta}_m + .3\dot{\theta}_m = 1 - \theta_L$

LOAD $.8\,\ddot{\theta}_L + .1\,\dot{\theta}_L = 0$

BACKLASH .3 RAD.

COMBINED SYSTEM TRAJECTORY

TRAJECTORY OF SYSTEM WITH LOAD SEPARATED

SEPARATION DIVIDING LINE

VELOCITY AND DISPLACEMENT OF SYSTEM WITHOUT LOAD AT RECOMBINATION

VELOCITY AND DISPLACEMENT OF SYSTEM AT RECOMBINATION

VELOCITY AND DISPLACEMENT OF LOAD DURING SEPARATION

VELOCITY AND DISPLACEMENT OF LOAD AT RECOMBINATION

Figure (27)

14. Conclusions.

By way of recapitulation, the eight considered cases were governed by the following equations.

Case I — Limit cycle: None

$$\ddot{\theta}_o + .8\dot{\theta}_o + \theta_o = 1$$
$$.6\ddot{\theta}_m + .48\dot{\theta}_m + \theta_m = 1$$
$$.4\ddot{\theta}_L + .32\dot{\theta}_L = 0$$

Case II — None

$$\ddot{\theta}_o + .2\dot{\theta}_o + \theta_o = 1$$
$$.5\ddot{\theta}_m + .2\dot{\theta}_m + \theta_m = 1$$
$$.5\ddot{\theta}_L = 0$$

Case III — 1.030

$$\ddot{\theta}_o + .2\dot{\theta}_o + \theta_o = 1$$
$$.5\ddot{\theta}_m + .2\dot{\theta}_m = 1 - \theta_L$$
$$.5\theta_L = 0$$

Case V — .52

$$\ddot{\theta}_o + .4\dot{\theta}_o + \theta_o = 1$$
$$.5\ddot{\theta}_m + .1\dot{\theta}_m = 1 - \theta_L$$
$$.5\ddot{\theta}_L + .3\theta_L = 0$$

Case VI — .550

$$\ddot{\theta}_o + .4\dot{\theta}_o + \theta_o = 1$$
$$.5\ddot{\theta}_m + .3\dot{\theta}_m = 1 - \theta_L$$
$$.5\ddot{\theta}_L + .1\dot{\theta}_L = 0$$

Case IV — 1.150

$$\ddot{\theta}_o + .2\dot{\theta}_o + \theta_o = 1$$
$$.2\ddot{\theta}_m + .2\dot{\theta}_m = 1 - \theta_L$$
$$.8\ddot{\theta}_L = 0$$

Case VII — .250

$$\ddot{\theta}_o + .4\dot{\theta}_o + \theta_o = 1$$
$$.2\ddot{\theta}_m + .1\dot{\theta}_m = 1 - \theta_L$$
$$.8\ddot{\theta}_L + .3\dot{\theta}_L = 0$$

Case VIII — .466

$$\ddot{\theta}_o + .4\dot{\theta}_o + \theta_o = 1$$
$$.2\ddot{\theta}_m + .3\dot{\theta}_m = 1 - \theta_L$$
$$.8\ddot{\theta}_L + .1\dot{\theta}_L = 0$$

Systems were grouped in the above order so that similar inertia ratios could be inspected as a group.

When backlash is outside the feedback loop, the system is ultimately stable and does not limit cycle, however it is subject to a residual steady state error in response to a step input, which error may be as great as the magnitude of the backlash.

When backlash is enclosed in the feed back loop, a limit cycle will invariably result providing the system possesses viscous friction only.

The majority of cases considered exhibited $\theta_L \dot{\theta}_L, \theta_o \dot{\theta}_o$ lines for recombination which approached the origin from slopes of opposite sign, as in the following example.

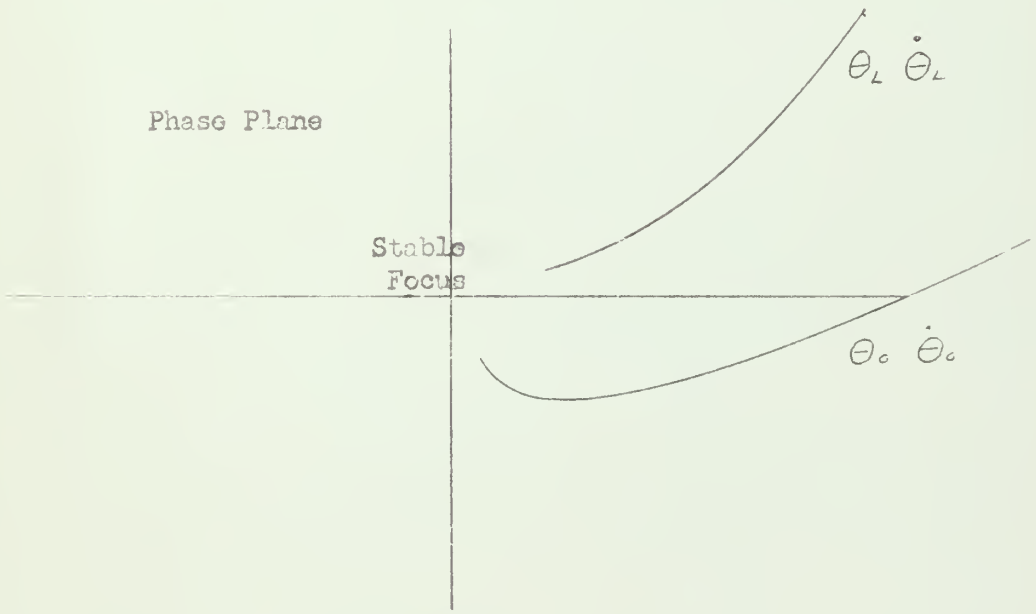

Figure (28)

It was originally believed that this difference in slopes was a necessary condition for the existence of a limit cycle and that the minimum value of the $\theta_o \dot{\theta}_o$ line was an indication of the magnitude of the limit cycle. Neither of these is the case. The limit cycle was always found to occur outside of the minimum value of the $\theta_o \dot{\theta}_o$ line. Case VIII showed the following configuration for the $\theta_L \dot{\theta}_L$, $\theta_o \dot{\theta}_o$ lines in the neighborhood of the origin.

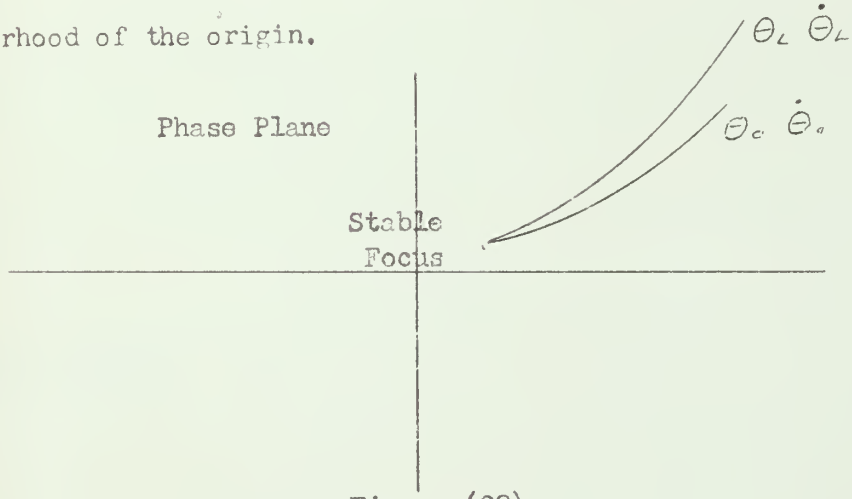

Figure (29)

This is not inconsistent with previously considered cases and is simply an indication that the decrease in momentum for both load and open loop system are equal for decreasing values of $\dot{\theta}_{mo}$

The position of the system without the load, at recombination, for various initial separation values of $\dot{\theta}_{mo}$ possesses a characteristic downward bow as in the following:

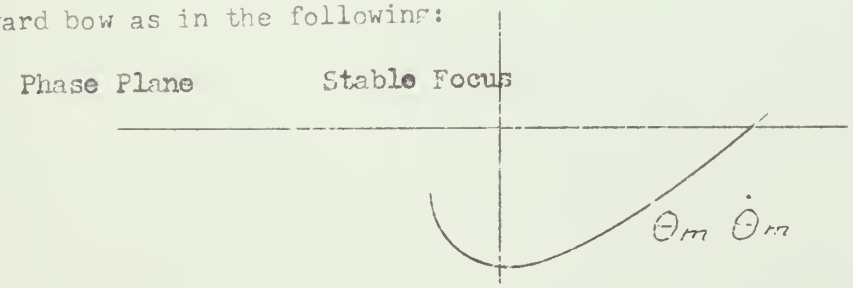

Figure (30)

It was originally believed that there might be some correlation between the existence and magnitude of the limit cycle and the position of minimum value of the $\theta_m \dot{\theta}_m$ recombination line, however no correlation was found to exist.

The shape and location of this $\theta_m \dot{\theta}_m$ line varied from system to system with varying frictional and inertia distributions, however it always possessed a minimum value and its most characteristic feature was the upward hook in the third quadrant which corresponded to small initial $\dot{\theta}_{mo}$ values for the separated trajectories.

Of most significance are the graphs shown as figures (31) and (32). Figure (31) is a plot of the magnitude of the limit cycle versus the $\frac{\text{Friction of Load}}{\text{Friction of System}}$ ratio when (a) the inertia of the load (J_L) was equal to the inertia of the system without the load (J_m) and when (b), $J_L = 4 J_m$ The steep upward slope of the magnitude of the limit cycle with decreasing F_L/F_o values is of interest, clearly demonstrating that the change in frictional effects in the load is much more pronounced when the load possesses the greater part of the inertia. This is illustrated by the fact that the $J_L = 4J_m$ line crosses the $J_L = J_m$ line at low values of F_L/F_o .

Figure 32 is a plot of the magnitude of the limit cycle versus the J_L/J_m ratio for three different frictional distributions. This graph presents the same information as figure (31) but in a different manner. Most noteworthy is the change in slope of the $\frac{J_L/J_m}{\text{magLim Cyc}}$ line with change in frictional distribution. When the load possesses the greater part of the friction, an increase in the J_L/J_m ratio decreases the limit cycle

whereas when the load possesses considerably less damping than the system, an increase in the magnitude of the limit cycle is the result of increasing the J_L/J_m ratio.

The overall system damping is seen to have the most effect in moving the $\frac{J_L/J_m}{mag.\ lim.\ cyc.}$ curves upward or downward while the individual F_L/F_m ratios determine the slope of those curves.

From this, the following generalizations for design may be made for the purpose of minimizing the magnitude of the limit cycle:

If the system damping is small, $2\zeta\omega_n \leq .2$, the J_L/J_m ratio should be made as small as possible when backlash is included inside the feedback loop.

If the system damping is somewhat greater, $2\zeta\omega_n \geq .4$, the J_L/J_m ratio should be made large, and a further reduction in the limit cycle may be achieved by placing the preponderance of damping in the load. This is quite feasible, and would be the case when a tachometer used in feedback is attached directly to the output shaft.

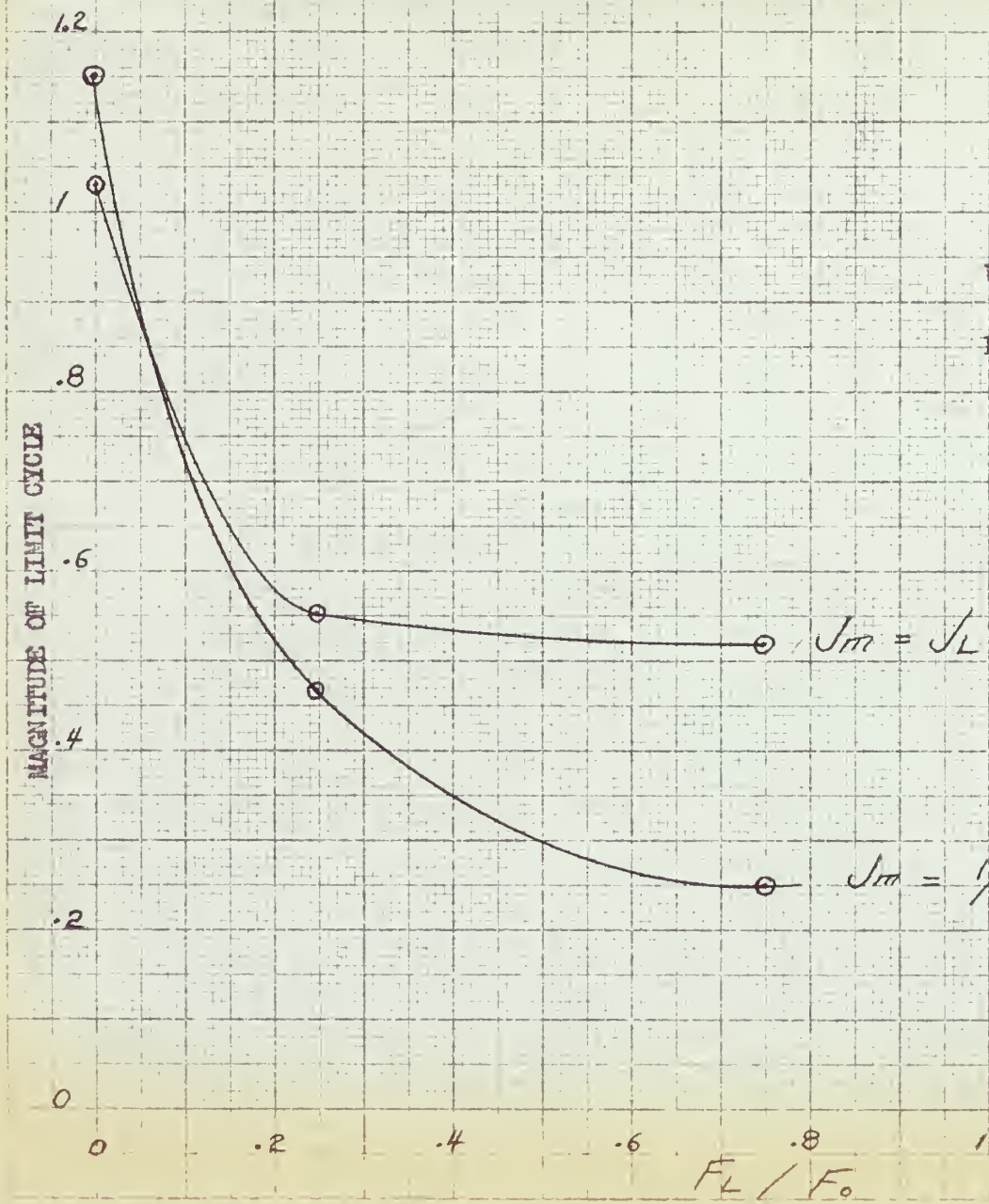

VARIATION OF MAGNITUDE OF LIMIT CYCLE WITH VARIATION OF RATIO OF $\frac{\text{LOAD DAMPING}}{\text{SYSTEM DAMPING}}$ FOR INERTIA DISTRIBUTIONS: $J_m = J_L$, $J_m = 1/4\ J_L$

Figure (31)

whereas when the load possesses considerably less damping than the system, an increase in the magnitude of the limit cycle is the result of increasing the J_L/J_m ratio.

The overall system damping is seen to have the most effect in moving the $\frac{J_L/J_m}{mag.\ lim.\ cyc.}$ curves upward or downward while the individual F_L/F_m ratios determine the slope of those curves.

From this, the following generalizations for design may be made for the purpose of minimizing the magnitude of the limit cycle:

If the system damping is small, $2\zeta\omega_n \leq .2$, the J_L/J_m ratio should be made as small as possible when backlash is included inside the feedback loop.

If the system damping is somewhat greater, $2\zeta\omega_n \geq .4$, the J_L/J_m ratio should be made large, and a further reduction in the limit cycle may be achieved by placing the preponderance of damping in the load. This is quite feasible, and would be the case when a tachometer used in feedback is attached directly to the output shaft.

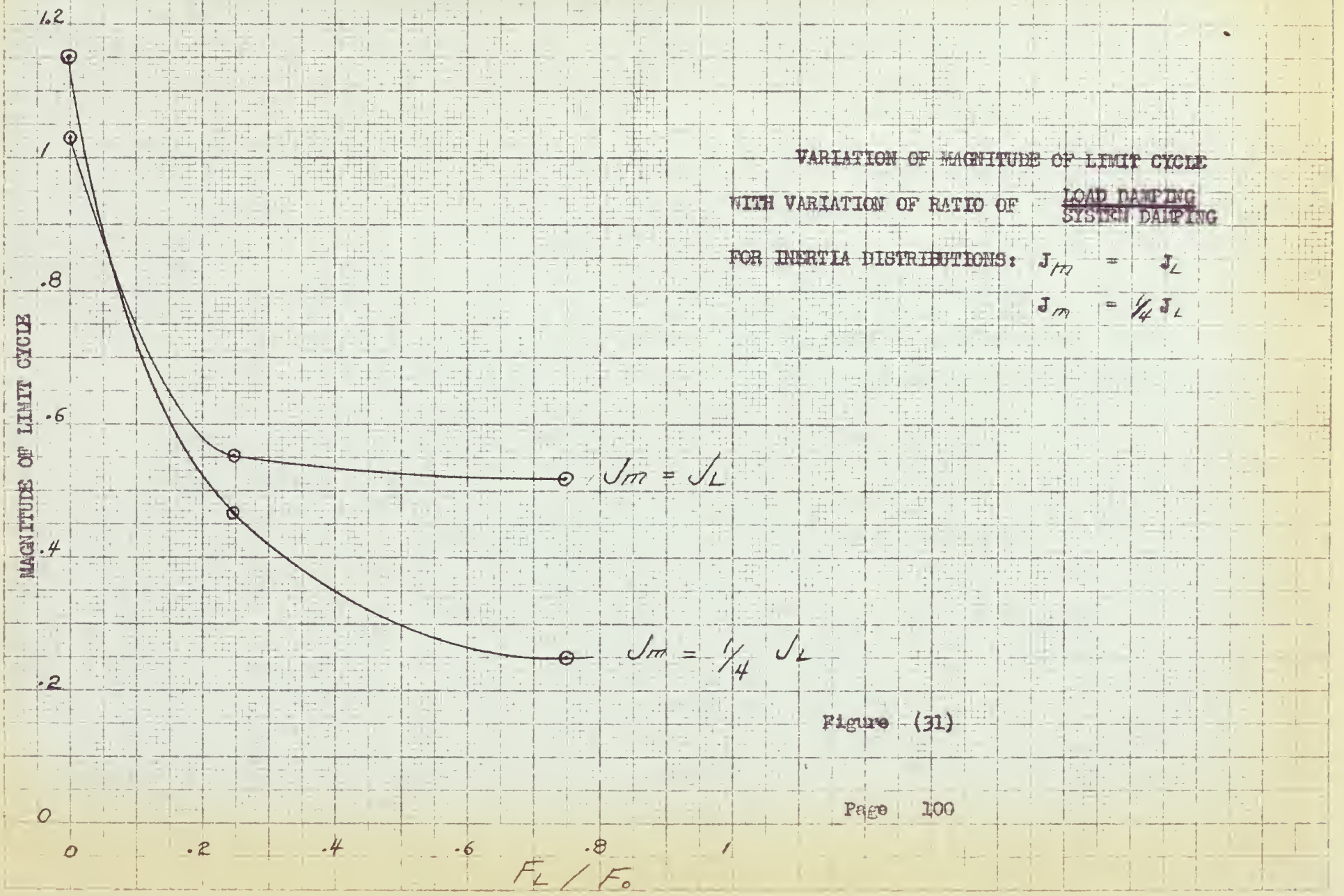
VARIATION OF MAGNITUDE OF LIMIT CYCLE
WITH VARIATION OF RATIO OF LOAD DAMPING / SYSTEM DAMPING
FOR INERTIA DISTRIBUTIONS: $J_m = J_L$
$J_m = 1/4\ J_L$
MAGNITUDE OF LIMIT CYCLE
1.2
1
.8
.6
.4
.2
0
$J_m = J_L$
$J_m = 1/4\ J_L$
0
.2
.4
.6
.8
1
F_L / F_o

Figure (31)

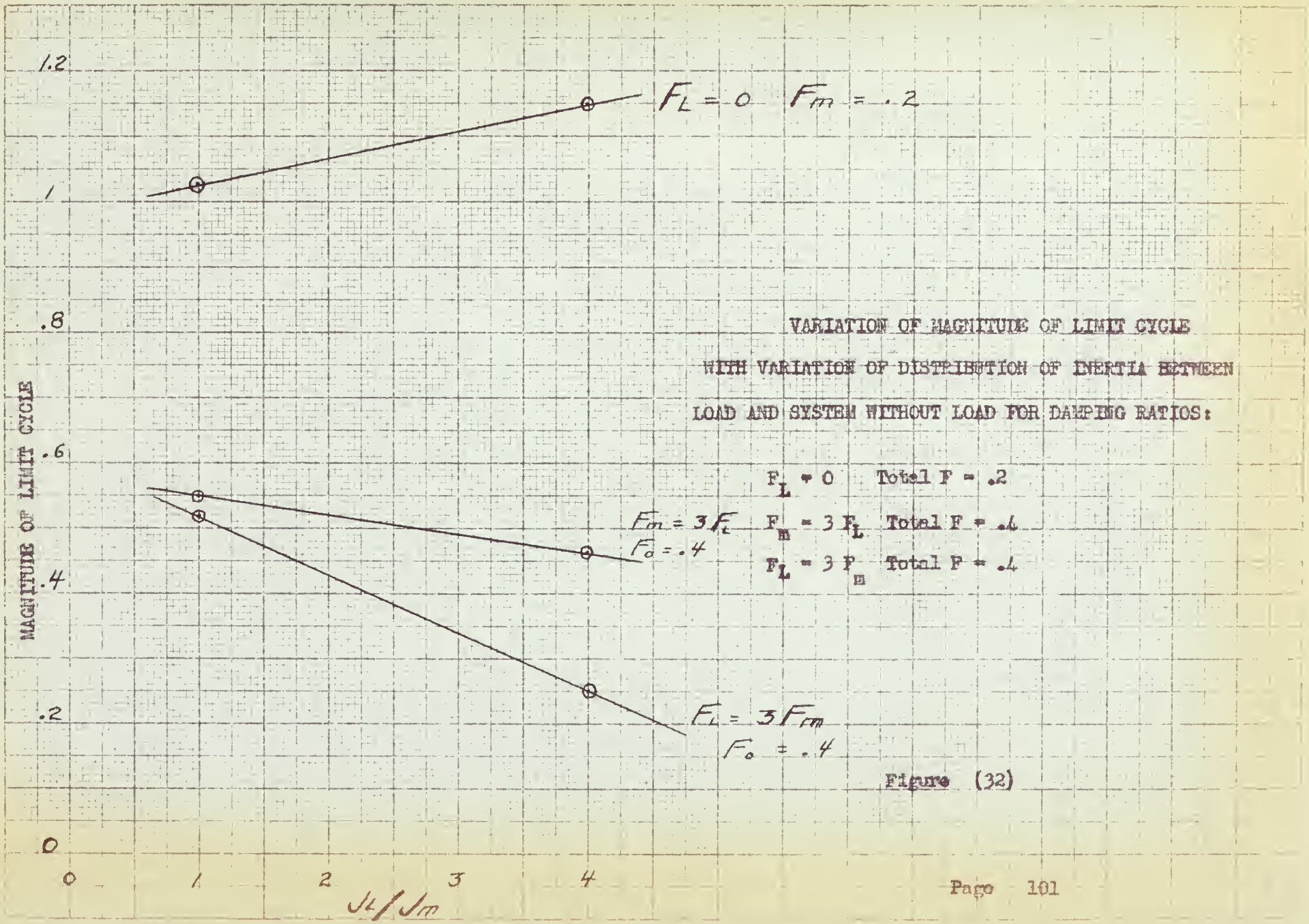

VARIATION OF MAGNITUDE OF LIMIT CYCLE WITH VARIATION OF DISTRIBUTION OF INERTIA BETWEEN LOAD AND SYSTEM WITHOUT LOAD FOR DAMPING RATIOS:

$F_L = 0$ Total F = .2

$F_m = 3F_L$ Total F = .4

$F_L = 3F_m$ Total F = .4

Figure (32)